

Advancing Frontiers in Bone Bioprinting

Nureddin Ashammakhi,* Anwarul Hasan, Outi Kaarela, Batzaya Byambaa, Amir Sheikhi, Akhilesh K. Gaharwar, and Ali Khademhosseini*

Three-dimensional (3D) bioprinting of cell-laden biomaterials is used to fabricate constructs that can mimic the structure of native tissues. The main techniques used for 3D bioprinting include microextrusion, inkjet, and laser-assisted bioprinting. Bioinks used for bone bioprinting include hydrogels loaded with bioactive ceramics, cells, and growth factors. In this review, a critical overview of the recent literature on various types of bioinks used for bone bioprinting is presented. Major challenges, such as the vascularity, clinically relevant size, and mechanical properties of 3D printed structures, that need to be addressed to successfully use the technology in clinical settings, are discussed. Emerging approaches to solve these problems are reviewed, and future strategies to design customized 3D printed structures are proposed.

alternatives; however, they often lack native tissue-mimicking structure, which may cause them to fail to properly integrate in the recipient sites. Thus, new bone engineering strategies such as three-dimensional (3D) bioprinting may help to produce constructs that can closely represent anatomic features of the native bone,^[1–5] and improve implant outcome

Bone is a complex heterogeneous tissue with distinctive structural and mechanical properties and it has hierarchical organizational levels.^[6] Bone is also a dynamic structure that undergoes continuous remodeling in response to various demands. Bone is connected to

blood vessels in the periosteum by transverse channels, which make bone a highly ordered and vascularized tissue. Bone healing involves mesenchymal stem cell (MSC) migration and, then bone formation.^[7] During regeneration, biomolecules are released from the extracellular matrix (ECM), and ECM remodeling is coordinated until complete bone healing is achieved.^[8] These details of structure and function should be carefully considered when a 3D-bioprinted bone-biomimetic constructs is developed.^[9]

1. Introduction

Bone defects resulting from congenital abnormalities, trauma, disease, or surgical resection require reconstruction by using customized grafts to restore structure and function. The current standard of using autografts and allografts, suffers from multiple problems, including limited supply, risk of complications, immune reactions and the transmission of infectious agents. Synthetic biomaterials have been developed as

Prof. N. Ashammakhi, Dr. A. Sheikhi, Prof. A. Khademhosseini
Center for Minimally Invasive Therapeutics (C-MIT)
University of California – Los Angeles
Los Angeles, CA 90095, USA
E-mail: n.ashammakhi@ucla.edu; khademh@ucla.edu

Prof. N. Ashammakhi, Prof. A. Khademhosseini
California NanoSystems Institute (CNSI)
University of California – Los Angeles
Los Angeles, CA 90095, USA

Prof. N. Ashammakhi, Prof. A. Khademhosseini
Department of Bioengineering
University of California – Los Angeles
Los Angeles, CA 90095, USA

Prof. N. Ashammakhi, Dr. O. Kaarela
Division of Plastic Surgery
Department of Surgery
Oulu University Hospital
Oulu FI-90014, Finland


Prof. A. Hasan
Department of Mechanical and Industrial Engineering
College of Engineering
Qatar University
Doha 2713, Qatar

Prof. A. Hasan
Biomedical Research Center
Qatar University
Doha 2713, Qatar

Dr. B. Byambaa
Center for Biomedical Engineering
Department of Medicine
Brigham and Women's Hospital
Harvard Medical School
Cambridge, MA 02115, USA

Dr. B. Byambaa
Harvard-MIT Division of Health Sciences and Technology
Massachusetts Institute of Technology
Cambridge, MA 02139, USA

Prof. A. K. Gaharwar
Department of Biomedical Engineering
Department of Materials Science and Engineering
and Center for Remote Health and Technologies
Texas A&M University
College Station, TX 77841, USA

 The ORCID identification number(s) for the author(s) of this article can be found under <https://doi.org/10.1002/adhm.201801048>.

DOI: 10.1002/adhm.201801048

Recently, 3D printing technology has been used to produce 3D scaffolds that can be seeded with cells.^[10,11] Three-dimensional bioprinting has advanced bone tissue fabrication further by loading cells and bioactive cues directly into the bioink to produce constructs that have controlled patterns and biomimetic structure.^[9,12,13] Bioprinting has the potential to enable the development of custom-made constructs for personalized treatment.^[14] In addition, it has many other advantages that include a) eliminating the need for cell seeding of scaffolds and inhomogeneous cell distribution,^[15] b) precise control over the porosity, pore size, and pore interconnectivity in the construct,^[16] and c) accurate deposition of biomaterials and cells in predetermined architectures that include features such as a vascular network to improve construct-tissue integration.

Three-dimensional bioprinting makes it also possible to produce constructs intraoperatively.^[17] This is especially important in cases where the defect size and shape cannot be determined preoperatively, such as may occur following debridement of injured joints.^[18] The procedure can also be useful in the reconstruction of complex craniomaxillofacial (CMF) defects,^[19] where imaging-based bioprinting [employing magnetic resonance imaging (MRI) or computed tomography (CT)] can be used to construct grafts that can fit precisely into CMF bone defects.

Recent interest in developing customized biomimetic scaffolds for regenerative therapeutics stimulated research for the production of complex cell-laden 4D constructs using bioresponsive materials. To this end, Ionov has reviewed recent advances in developing materials and methods used for 4D biofabrication of a variety of tissues, such as in situ blood vessel formation.^[20] In a prospective review, Placone and Engler have discussed the recent advances in extrusion-based 3D printing and bioprinting discussing the use of single- and multimaterial based extrusion, which can be useful for the engineering of tissue interfaces.^[21] Moreover, current 3D bioprinting methods have been thoroughly reviewed and the limitations of biomaterials in terms of printability, material materials compatibility, and cell viability have been discussed in a recent paper^[22] by Lee and Yeong who have also discussed the pivotal bioprinting design factors, including material heterogeneity, shape and resolution, and cellular-material remodeling dynamism in direct bioprinting, in-process crosslinking, postprocess crosslinking, indirect bioprinting, and hybrid bioprinting. Furthermore, in a review by Chawla et al. the use of silk fibroin as bioink was discussed covering both silkworm and spider silk, their uses in 3D printing and cell interactions including the modulation of cell signaling.^[23] These reviews expand our knowledge about the 3D printing and bioprinting and will help expand their applications.

The present review is focused on bone 3D bioprinting and compliments these reviews, in an important niche and rapidly advancing area. This paper discusses critically the state-of-the-art in 3D bioprinting technologies, with a focus on bone reconstruction, and it integrates knowledge gained from in vitro and in vivo studies combined with clinical insight. We have also evaluated various bioprinting methods, commonly used bioinks, bioactive additives such as osteoconductive and osteoinductive elements used specifically for 3D printing of bone



Nureddin Ashammakhi is focusing on translational tissue regenerative therapy. Currently, he is working on 3D bioprinting and organ-on-a-chip models for regenerative and personalized medicine. He is an expert in bioabsorbable, nanofibrous, and drug release implants. He was previously a professor

of biomaterials technology in Tampere University of Technology, Finland, Chair of regenerative medicine, Keele University, UK and Adjunct Professor in Oulu University, Finland before he joined UCLA as a visiting professor, and now as Associate Director of the Center for Minimally Invasive Therapeutics.



Anwarul Hasan is the Director of the Nano Microscale Technologies and Tissue Engineering Lab, and an Assistant Professor in the Department of Mechanical and Industrial Engineering and Biomedical Research Center at Qatar University. Earlier he was a Visiting Assistant Professor at Harvard Medical School, and

Massachusetts Institute of Technology (MIT), USA and an Assistant Professor at the American University of Beirut in Lebanon from 2014 to 2017.



Ali Khademhosseini is the Levi Knight Professor of Bioengineering, Chemical Engineering and Radiology at UCLA. He is the Founding Director of the Center for Minimally Invasive Therapeutics at UCLA. Previously, he was a Professor of Medicine at Harvard Medical School. He is recognized as a leader

in combining micro- and nanoengineering approaches with advanced biomaterials for regenerative medicine applications.

tissue. The current challenges and potential solutions in the field of bone bioprinting are discussed. Future prospects of bone 3D bioprinting are analyzed, and emerging translational technologies are outlined.

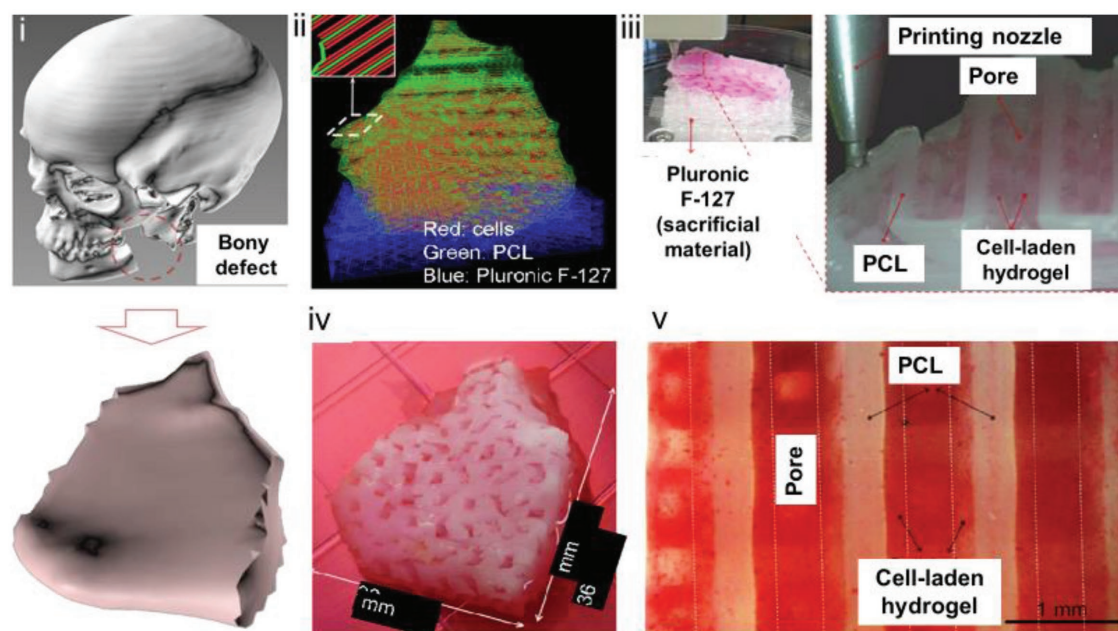


Figure 1. Reconstruction of a human mandible graft. i) 3D CAD model obtained from CT image data. ii) Construction of the bone defect 3D architecture using CAM software: green, blue, and red lines represent the paths used to dispense various inks (PCL, Pluronic F-127, and cell-laden hydrogel, respectively). iii) 3D printing: enlarged view shows the patterning of a construct layer. iv) Image of a 3D printed construct cultured in osteogenic medium for 28 days. v) hAFSC osteogenic differentiation in the printed construct was confirmed by Alizarin Red S staining (indicating calcium deposition). Reproduced with permission.^[25] Copyright 2016, Nature Publishing Group.

2. Bioprinting

Three-dimensional bioprinting can utilize imaging techniques such as CT or MRI to reproduce the structural features of the target tissue, and appropriate biomaterials and cells to produce 3D implants for the reconstruction of bone defects.^[24] For example, employing computer-aided design and computer-aided manufacturing (CAD-CAM) it was possible to produce complex 3D images for bioprinting.^[25] The bioink which is used to print the structure is usually a cell-laden hydrate polymer network, which is fed into the printer (Figure 1). Subsequently, printed constructs are maintained

in culture for maturation, followed by transplantation to the target site.

2.1. Bioprinting Techniques

Three-dimensional bioprinting is commonly performed using one of the following techniques (Figure 2A–C): 1) microextrusion, 2) inkjet, and 3) laser-assisted bioprinting (LAB).^[24,26] In microextrusion 3D printing, bioink is extruded through nozzle(s) either by pneumatic or mechanical methods (piston or screw) (Figure 2A).^[27] In inkjet bioprinting, thermal, piezoelectric,

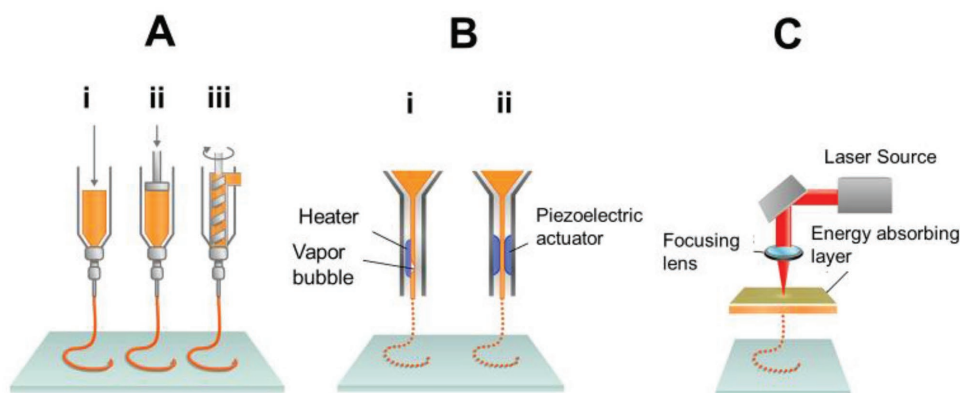


Figure 2. Three-dimensional bioprinting techniques. The three most common 3D bioprinting techniques: A) microextrusion, B) inkjet, and C) laser-assisted bioprinting. The microextrusion technique can be of three types, namely, i) pneumatic, ii) piston based mechanical, and iii) screw-based mechanical techniques while the inkjet technique can be either thermal or piezoelectric type. (A,B) Adapted with permission.^[177] Copyright 2013, Wiley-VCH. (C) Adapted with permission.^[13] Copyright 2017, Nature Publishing Group.

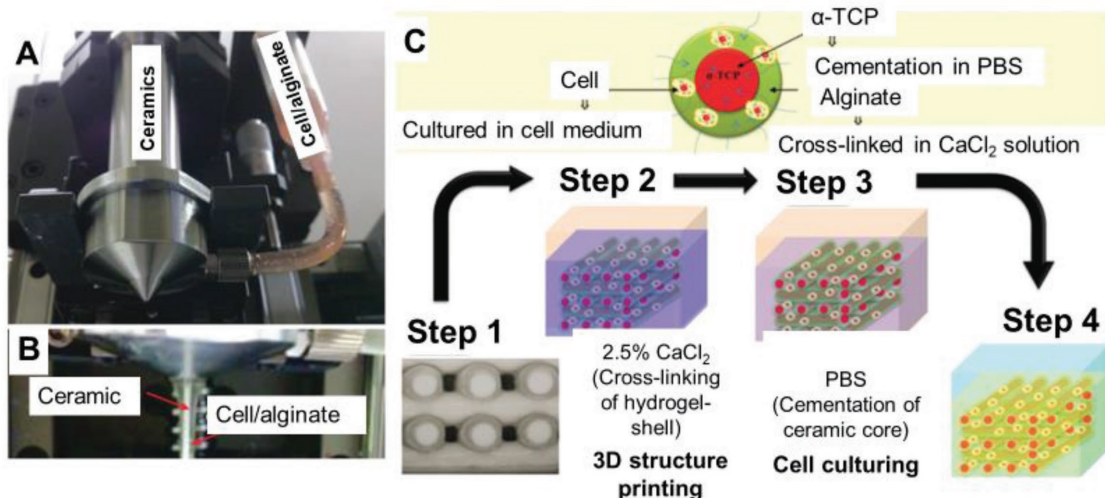


Figure 3. Images of dual extrusion printing. A) Two inks are separately extruded and combined after their exit from independent orifices to produce a core shell construct (A and B). Constructs with a ceramic (α -TCP) core and cell-laden alginate hydrogel shell are shown. Following bioprinting, the construct is immersed in CaCl_2 for crosslinking, followed by cementation of the α -TCP core in PBS. The hardened construct is then transferred to cell culture C). (A–C) Reproduced with permission.^[29] Copyright 2016, The Royal Society of Chemistry.

or electromagnetic means are used to deposit small bioink droplets through nozzle(s) (Figure 2B). In laser-assisted bioprinting (LAB), laser energy is used to volatilize a sacrificial layer, propelling a payload to a receiving substrate (nozzle-free bioprinting) (Figure 2C).^[28] In addition, microextrusion can employ multiple nozzles, especially for printing materials under harsh conditions that can be harmful to cells. For example, two types of ink can be printed separately and then combined to produce core-shell structures, wherein the core can be a ceramic, e.g., alpha tricalcium phosphate (α -TCP) and the shell can be a cell-laden alginate hydrogel (Figure 3).^[29] Separate printing can also be used for producing a reinforcement structure from one outlet and a cell-laden hydrogel from a second outlet.^[25] Recently, stereolithography (SLA) was used to incorporate cells into printed structures.^[30–32] SLA involves the use of a

ultraviolet (UV) light beam on a liquid photopolymer, leading to polymer crosslinking and layer-by-layer printing.^[33] Hybrid systems, in which hard and soft components can be combined by using extrusion bioprinting and SLA, have also been developed (Figure 4).^[34] More recently, microfluidic bioprinting was developed by combining microfluidic print-heads with extrusion printing for high velocity printing of multiple materials (Figure 5A).^[35] This new modality makes it possible to program sequential or simultaneous extrusion of different bioinks^[36–38] with complex spatiotemporal control such as printing of gradients into structures. With microfluidics, it is also possible to achieve single-cell encapsulation into microgels.^[39–41] Such microgels can be used for bioprinting and they may also help to prolong the residence times of delivered cells and soluble factors in vivo.^[40]

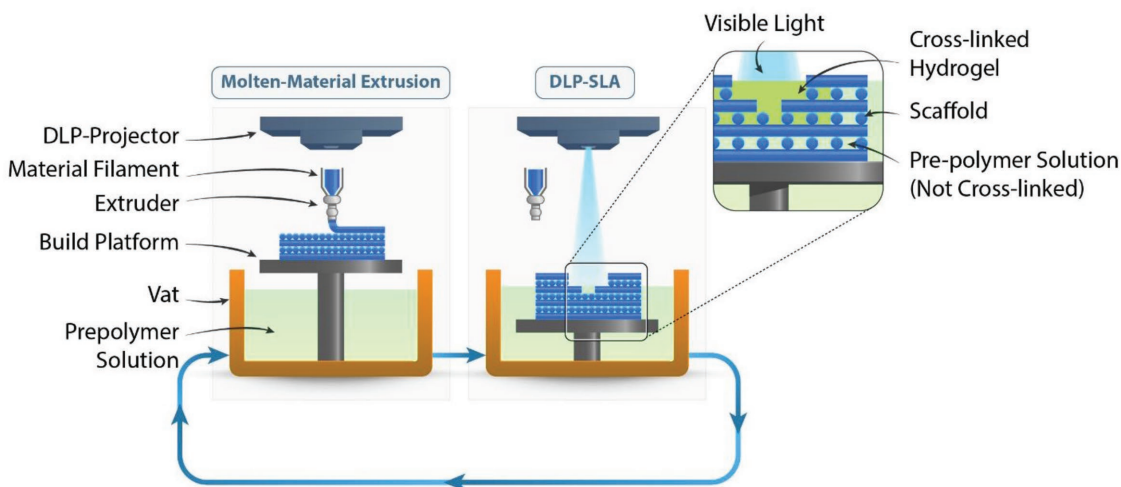


Figure 4. Hybrid bioprinter combining extrusion and SLA printing. Schematic illustration of combinatorial molten-material extrusion and digital light processing-based stereolithography (DLP-SLA) processing with a hybrid scaffold-hydrogel construct during fabrication. Reproduced with permission.^[34] Copyright 2015, IOP Publishing Group.

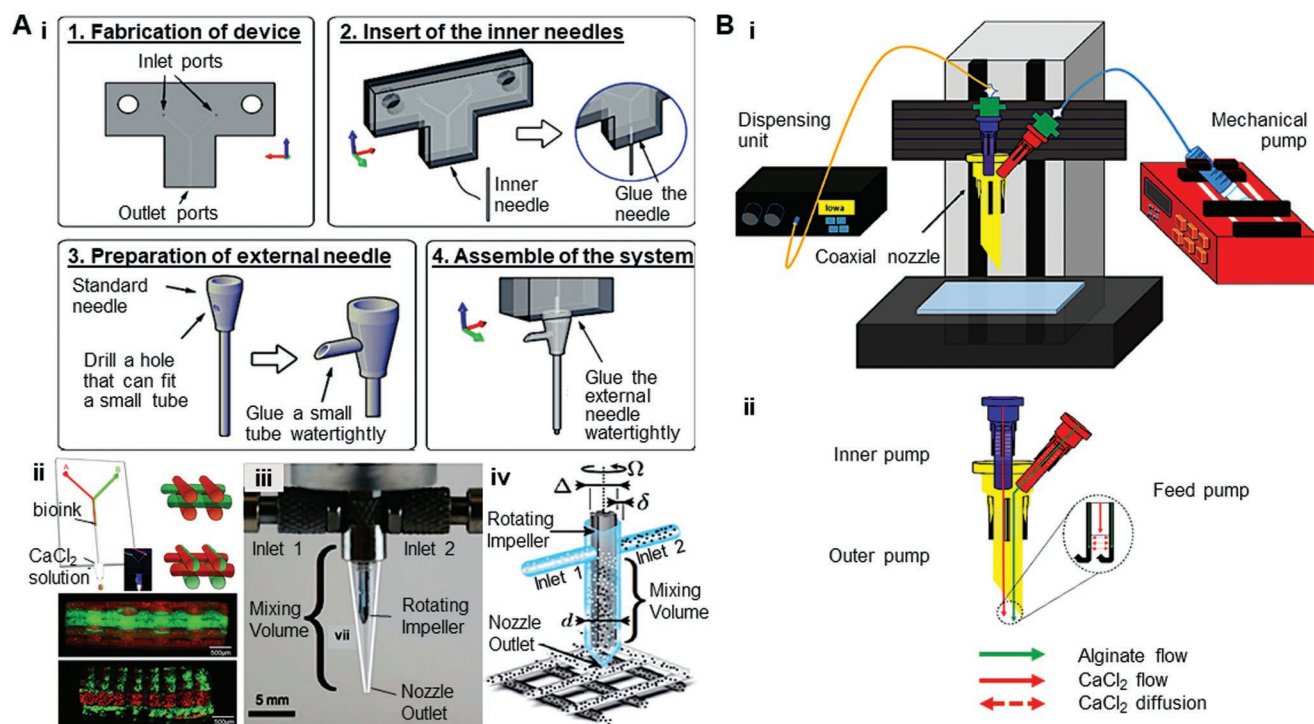


Figure 5. Microfluidic A) and coaxial B) bioprinting. A-i) Schematic illustration of various steps of fabrication of microfluidic printing device. ii) Illustration of a microfluidic system that allows the flow of two different bioinks (red and green) through a single channel. Inset photograph shows the coaxial needle system. Schematic diagram and fluorescence microscopy image of a cross-sectional view of a 3D constructs that were produced with either alternate deposition or alternate/simultaneous deposition, are also shown. iii) Image of the impeller-based active mixer. White lines were added to accentuate the edges of the nozzle tip. iv) Schematic illustration of a mixing nozzle for 3D printing of two different inks. Each ink enters through an independent inlet into the mixing chamber, which has a defined diameter (d). The ink is homogenized in a narrow gap having a defined width (δ) by an impeller of defined diameter (Δ) rotating at a fixed rate (Ω). B) Printing of alginate tubes using a coaxial extrusion printing system. i) Schematic illustration of the 3D printing system (using a mechanical pump). Sodium alginate (blue line) and CaCl_2 (yellow line) are delivered to the 3D printing system. ii) Illustration of the coaxial nozzle. Sodium alginate solution flows through the sheath, and CaCl_2 solution flows through the core. (A-i) Reproduced with permission.^[42] Copyright 2017, Springer. (A-ii) Reproduced with permission.^[38] Copyright 2016, Wiley-VCH. (A-iii) Reproduced with permission.^[36] Copyright 2015, PNAS publishing group. (B) Reproduced with permission.^[99] Copyright 2017, Springer.

The advantages and disadvantages of different bioprinting modalities are summarized in **Table 1**. Although the resolution of microextrusion bioprinting is 50–500 μm ,^[27,42] it can be improved to reach values of <50 μm ^[42] by combining microfluidics with the system. Extrusion method is however, associated with shear-stress during printing which may affect cell viability.^[43] On the other hand, inkjet printing is a low-cost technique and can achieve resolutions close to 50 μm with precise deposition of cells and biomaterials.^[26] The key advantage of inkjet bioprinting is speed; its deposition rates range from 1 to 10 000 droplet s^{-1} .^[44] Heat and mechanical stress involved in inkjet printing may damage cells.^[45] However, such heating was not found to have any significant effect on cell apoptosis, because cooling of the printed structure to room temperature occurs within seconds.^[46] For example, bioink drops are heated in the print head to $\approx 45^\circ\text{C}$ for less than 2 μs , resulting in an average cell viability of $\approx 90\%$.^[46] Moreover, with the introduction of mechanical valves and the printing of highly viscous cell-containing hydrogel precursors, cell viability has been significantly improved.^[47] While LAB is known for its excellent resolution, it is associated with lower throughput and it is slower than the inkjet and extrusion techniques. When it is used for bioprinting of mesenchymal stem cell (MSC)

grafts, laser-induced forward transfer (LIFT) can preserve the graft structure.^[48] SLA is characterized by accuracy, high resolution, and control of its internal and external architecture.^[49] For example, a high-resolution projection SLA apparatus allows patterning at a <5 μm resolution.^[50] However, its use is limited by cost and maintenance constraints.^[49] Concern about UV inducing mutations is being addressed by developing an SLA that employs visible light for bioink crosslinking.^[51]

3. Bone Biofabrication Parameters and Requirements

A range of parameters dictates 3D bone bioprinting process, including the formulation of bioinks, crosslinking mechanism, mechanical properties, cells, and bioactive cues including osteoinductive agents. In this section, we will discuss different aspects of biofabrication parameters that may affect the performance of 3D printed constructs applied for bone regeneration. Specifically, we will discuss requirements for bioink for 3D printing, including the type of polymer, crosslinking mechanism, and bioactive additives. Osteoinductive agents added to bioink to control and direct cell functions will also be discussed.

Table 1. Comparison of bioprinting methods. Adapted with permission.^[24] Copyright 2014, Nature Publishing Group.

	Bioprinter type		
	Inkjet	Microextrusion	Laser assisted
Material viscosities	3.5–12 mPa s ⁻¹	30 mPa s ⁻¹ to $> 6 \times 10^7$ mPa s ⁻¹	1–300 mPa s ⁻¹
Gelation methods	Chemical, photo-crosslinking	Chemical, photo-crosslinking, shear-thinning, temperature	Chemical, photo-crosslinking
Preparation time	Short	Short to medium	Medium to long
Print speed	Fast (1–10 000 droplets s ⁻¹)	Slow (10–50 μ m s ⁻¹)	Medium-fast (200–1600 mm s ⁻¹)
Resolution or droplet size	<1 pL to >300 pL droplets, 50 μ m wide	5 μ m to millimeters wide	Microscale resolution
Cell viability	>85%	40–80%	>95%
Cell densities	Low, < 10 ⁶ cells mL ⁻¹	High, cell spheroids	Medium, 10 ⁸ cells mL ⁻¹
Printer cost	Low	Medium	High
Advantages ^[170]	high speed, availability, relatively low cost	High viscosity bioinks may be used and high cell densities can be printed	Precise fabrication and fast printing
Disadvantages ^[170]	Lack of precise droplet size and placement, requirement for low viscosity bioinks	Distortion of cell structure and often low resolution	High intensity UV light and long post-processing are often required. Also, many of the inks are not biocompatible

We will also evaluate the role of cells and microenvironment in directing bone regeneration. It is expected that optimizing these parameters will help in designing optimal 3D printed constructs for bone regeneration.

3.1. Bioink Requirements

Bioink is the substance used to produce 3D printed constructs and it comprises a cell laden biomaterial with or without other additives. The selection of the biomaterial for use in bioink depends on a range of characteristics, including its chemical, physical, and biological properties. Specifically, the biomaterial should be printable and crosslinkable to achieve a stable construct structure after printing. The biomaterial should maintain its mechanical properties to support resulting 3D printed construct and allow tissue regeneration. It should also be cytocompatible (nontoxic in itself, its degradation products, or its metabolites). In addition to cells, bioactive molecules may also be included in the bioink and their spatial distribution can be controlled as required, e.g., into gradients to influence cell migration and differentiation to desired phenotypes. The biomaterial should also be able to support cell proliferation and formation of appropriate ECM. The biomaterial should have a fluid state to enable printing, and capability to subsequently gelate to form a solid structure. However, it should not gelate so quickly as this may lead to clogging the nozzle.^[32] Bearing in mind these requirements, various biomaterials can be employed in 3D bioprinting.

There are many biomaterials that were investigated for tissue engineering, but only a few are suitable for 3D bioprinting. For example, thermoplastics such as polylactide (PLA) and poly- ϵ -caprolactone (PCL) have excellent biocompatibility, but they are not suitable for 3D bioprinting due to their high processing (melting) temperature (poly-L-lactide, PLLA has a melting temperature of 173–178 °C and PCL has a melting temperature of 60 °C). Therefore, hydrated networks of polymers known as hydrogels are used for bioprinting.^[53] Suitable hydrogels

should be stable at physiological temperature to allow tissue formation and maturation. The extrudability of a polymeric solution depends on the biomaterial and on the printing system which can be modulated. In general, biomaterials with viscosities of 30 to $> 6 \times 10^7$ mPa s⁻¹ are considered suitable for 3D bioprinting by extrusion.^[24]

3.2. Polymers for Bioprinting

Alginate is the most commonly used hydrogel for bioprinting due to its low cost, biocompatible nature, high viscosity, and fast gelation kinetics. In bone bioprinting, alginate has been used alone^[29,56,64–67] or in combination with other biomaterials^[9,13,15,18,25,30,52,54,57,62,66–77] (Table 2). However, alginate suffers from low bioactivity,^[29] and thus, other polymers that have better bioactivity such as collagen were explored. Collagen is an interesting polymer that can promote cell adhesion. Unfortunately, it has low viscosity and slow gelation kinetics, and thus, it has been used only in few bone bioprinting studies.^[52] Composite hydrogels containing collagen and other biomaterials such as agarose were tested.^[72] The use of denatured form of collagen, gelatin, has also been explored in various combinations with other biomaterials. Another natural polymer, hyaluronic acid (HA), has been evaluated for bioprinting,^[25] but, it suffers from poor mechanical properties. Hence, it has been used in bioprinting as viscosity enhancer in combination with other polymers.^[78,79]

Natural polymers can be modified to have new properties such as crosslinkability and thus, they can be turned suitable for developing printable and stable 3D constructs. For example, chemical modification of the backbone of HA with methacrylate was employed to produce photo-crosslinkable methacrylated HA (MeHA).^[71] Chemical crosslinking enables also having biomaterials with tunable mechanical properties and degradation characteristics.^[80] It was found that thiol-modification of HA using gold nanoparticles can also increase the stiffness of the hydrogel.^[81] The modified gelatin hydrogel, gelatin

Table 2. Summary of reports on 3D bone bioprinting, listed in chronological order. Different cell types and biomaterials were used, with or without added elements. Bioprinting was followed by crosslinking using different methods. Relevant outcomes and construct properties are presented. Cells used include mesenchymal stem cells (MSCs), human MSCs (hMSCs), human bone marrow-derived stem cells (hBMSCs), porcine BMSCs (pBMSCs), goat BMSCs (gBMSCs), rat BMSCs (rBMSCs), mouse BMSC (mBMSCs), inferior turbinate MSCs (TMSCs), human amniotic fluid-derived (hAFSCs), adipose tissue-derived mesenchymal stem cells (aMSCs), endothelial cells (ECs), human umbilical vein endothelial cells (HUVECs), goat endothelial progenitor cells (gEPCs), the preosteoblast cell line MC3T3-E1, the osteosarcoma osteoblast-like cell line SaOS-2, and porcine fat tissue stromal vascular fraction (SVF) derived cells. Various biomaterials were used, including alginate (Alg), collagen type I (Col I), hyaluronic acid (HA), gelatin methacryloyl (GelMa), methacrylated gelatin (Me-Gel), HA-methacrylate (HAMA), PEG dimethacrylate (PEGDMA), methacrylated HA (MeHA), polylactide (PLA), polylactide-co-glycolide (PLGA), poly-ε-caprolactone (PCL), polyethylene glycol (PEG), polyvinyl alcohol (PVA), and carboxymethyl cellulose (CMC). The osteoconductive elements used include hydroxyapatite (HAp), tricalcium phosphate (TCP), calcium polyphosphate (polyP · Ca²⁺), bioactive glass (BaG), biphasic calcium phosphate (BCP), calcium phosphate (CP), nano-BaG (nBaG), nano-HAp (nHAp), *n*-silicate, microparticles (m-particles), and extracellular matrix (ECM). Growth factors include bone morphogenetic protein 2 plasmid DNA (BMP-2 pDNA), collagen binding domain BMP-2 CBD-BMP-2, and vascular endothelial growth factor (VEGF). Bioprinting was achieved through extrusion (Extr), fused deposition modeling (FDM), 3D fiber deposition (3D FD), ink-jetting or laser-assisted bioprinting (LAB) (e.g., laser-induced forward transfer (LIFT), near infrared (NIR) pulsed laser beam), microfluidic and stereolithography (SLA) methods. Solidification was achieved using different methods, involving materials such as calcium ions (Ca), barium (Ba), or strontium (Sr). Calcium chloride (CaCl₂) was used to release calcium ions. In some studies, ultraviolet (UV) irradiation was used. The photoinitiator VA-086 was used for UV crosslinking. Times are presented in days (d) and weeks (wk). Outcome is noted, including cell viability (viab), fiber diameter (φ), sizes of constructs, dimensions such as height (ht), and strength in kilo Pascals (kPa).

Cell	Material	Method	Gelation	Comment	Size, structure, strength	Ref.
gBMSCs	Alg, Lutrol F127, PEO-PPOPEO (Poloxamer 407), Matrigel, agarose, methylcellulose	3D FD (Pneumatic Extr)	CaCl ₂	<ul style="list-style-type: none"> Best gelation with Alg and Lutrol. Lutrol only 4% viab @ 3 d. Possible to print two different cell populations. On Alg osteogenic differentiation @ 14 d of culture. 	20 × 20 × 2 mm	[62]
pBMSCs	Temporary use of hydrogel (plasma + Alg) for 2 wks in culture. Then, cell grafts were removed.	LIFT	CaCl ₂	<ul style="list-style-type: none"> Possibility to use high cell density. High cell density increased differentiation. No difference in proliferation between printed and control cells. Generated 3D constructs of nondifferentiated and predifferentiated MSCs, which could be differentiated to bone and cartilage tissue grafts. Differentiated constructs kept their predefined shape even after several weeks in culture. 	Grids	[48]
gBMSCs and gEPCs	2 phases. Matrigel or Alg BCP m-particles. Lutrol (F127)	Pneumatic Extr	CaCl ₂ for Alg	<ul style="list-style-type: none"> ECs and MSCs viab and distinct cell distribution were maintained @ 2w. Cells homogeneously distributed throughout the gel. In mice, integration with the host tissue and formation of microvessels in the EC-phase. Demonstrated for the first time that multiple printed cell types retain their functionality in vivo and produce respective ECM. 		[66]
hBMSCs	Alg and BCP particles	3D Fiber depos (pneumatic Extr)	CaCl ₂	<ul style="list-style-type: none"> Viab 89% ± 2% @ 5 h, 88% ± 6% @ 24 h postprinting Uniform cell distribution Limited construct height achieved (10 layers). Cells remained in their planned compartment. MSC osteogenic differentiation. Tissue formed in vitro and in vivo. Limited interaction between cells in the adjacent layers. Lack of abundant bone formation. 	<ul style="list-style-type: none"> Size: 1 × 2 cm Porosity 70–5% (macro-55–5%, and microporosity 20–5%). Vertical pores were regular throughout, whereas transversal pores fused. 	[64]
MC3T3-E1	Alg between PLA struts	Pneumatic Extr	CaCl ₂	<ul style="list-style-type: none"> Viab 84% @ 25 d. Proliferation Mechanically improved 	100% pore interconnectivity	[65]
MSCs	Alg + CP + BMP-2 DNA	3D FD (Bioscaffolder = pneumatic Extr)	CaCl ₂	<ul style="list-style-type: none"> Optimal concentration of Alg is 10 µg mL⁻¹ 	<ul style="list-style-type: none"> 10 successive layers (20 × 20 × 5 OR 10 × 10 × 5 mm). Degraded by 6 wk 	[56]
hMSCs	Alg /gelatin + HAp powder in different concentrations (0–8%)	Fab@Home 3D printer Model 2 (Extrusion)	2-step processing: thermal for agar + CaCl ₂ for Alg gelation	<ul style="list-style-type: none"> Viab > 84% 3 d HAp increased gel viscosity without increasing significantly elastic modulus, and did not affect cell viability 		[77]

Table 2. Continued.

Cell	Material	Method	Gelation	Comment	Size, structure, strength	Ref.
SaOS-2	Alg /gelatin + silica + nBaG	Pressure (Extr)	CaCl ₂	BaG enhanced proliferation + mineralization	13 mm; 1.5 mm ht	[75]
SaOS-2	Alg + gelatin. Then, over layer of polyP · Ca ²⁺ agarose	Pneumatic Extr (Bioplotter)	CaCl ₂ . Cooling for agar	Agar + Ca poly Po4 resulted in increased proliferation and mineralization and hardness. With increasing incubation Time, cylinder shape disintegrated. Mechanical stability lost after d5	Cylinders: 1.6–1.9 mm thick	[76]
hBMSCs	PEGDMA + nBaG and nHAp. Photoinitiator Irgacure 2959 (I-2959)	Thermal inkjet	Not indicated	– Viab 86.62 ± 6.02% @ 21 d. least cytotoxic. With HAp. – Significantly highest ALP (osteogenic differentiation) with HAp – Even distribution of cells – Suitable to construct osteochondral interface.	4 mm diam. Compression modulus: 358.91 ± 48.05 kPa @ 21 d.	[15]
hBMSCs	PLGA 85:15 + PEG blend 93.5:6.5 microparticles + CMC or Pluronic F-127.	Fab@Home 2 (mechanical Extr)		– Mechanical properties best @ higher viscosity. However, reduced cell viability. – @Carrier: solid ratio of 1.5:1 viab was 87% @d0 and 77% @d 1. – PL127 requiring larger ratios than CMC to achieve complete extrusion	6 mm ø, 12 mm ht. Yield stress: 1.22–1.15 MPa. Young's modulus. 54.4–57.3 MPa. Porosity: 10.8–12.4%. Mean pore size: 65.3–76.6 µm.	[69]
hBMSCs	Acrylated PEG + acrylated peptide	Inkjet		– Viab 87.9 ± 5.3%. – Excellent mineralization.	4 mm cylindrical	[68]
hTMSCs	Silk fibroin + gelatin	Multihead deposition (Pneumatic Extr)	Tyrosinase + sonication	– Multilineage differentiation – Viable in 8SF-15G-T over 1 mo culture,	Maintained stable 3D structure	[52]
SaOS-2	Alg + gelatin + ECM	Microfluidic	Ca, Ba, or Sr	Viab > 95%		[57]
rBMSCs	CBD-BMP-2-collagen microfiber-laden methacrylamide gelatin hydrogel	Screw-based Extr (customized printer)	UV	– Viab 91.8 ± 0.9% after printing, 92.1 ± 1.5% @d7 and 94.9 ± 1.6% @d28 – Cells distributed well in the gel. – CBD-BMP-2-collagen microfibers induced osteogenic differentiation within 14 d, more efficiently than osteogenic medium.	20 × 20 × 2 mm	[73]
hBMSCs	Col I and agarose (for mechanical stiffness)	Inkjet (Thermal)	Gelation @15–37 °C	– Viab > 98% @21 d. Cell spread, branch + osteogenic differentiation in less stiff constructs.		[72]
hAFSCs	Gel composite + TCP + PCL + Pluronic	Extr (FDM)	Thrombin	– ≥95% viab on day 0,	Mandible form	[25]
MC3T3-E1	Alg-TCP core-shell	Extr (Screw for core, pneumatic for shell)	CaCl ₂	Almost all viable.	Compression strength 3.2 MPa, Mod 10.92 MPa	[29]
haMSCs	10 wt% GelMa + 2 wt% HAMA + 0.5 wt% VA-086 (Photoinitiator) solution	Pressure Extr (100 kPa)	UV	Viab 97% @d1, improved @ d3 and 7		[18]
hHUVESs, hMSCs	GelMA + PLA fibers + VEGF peptide + BMP-2 peptide	Extr (FDM) for PLA phase +SLA for GelMA phase		Highly osteogenic construct with organized vascular networks was generated.	Cylinder (9 mm f, 4 mm thick)	[30]
MC3T3-E1	Col I + α-TCP	Pneumatic Extr @230 kPa.	Tannic acid	Viab > 91% @4 h. Significantly higher cell activities		[54]
hBMSCs	MeHA, 0.1% photoinitiator Irgacure 2959.	Piezoelectric inkjet (Bioscaf-folter)	UV	– Viab 64.4% @ 21. Methacrylation made HA printable. – Intrinsic HA osteogenicity led to excellent osteogenic differentiation	20 × 20 × 3 mm, lumbar scaffold 20 × 25 × 1 mm	[71]

Table 2. Continued.

Cell	Material	Method	Gelation	Comment	Size, structure, strength	Ref.
MC3T3	Alg + PVA + HAp (varying concentrations)	Extr (HyRel printer)	CaCl ₂	<ul style="list-style-type: none"> – Viab 95.6% after print and 77.5% after Ca bath. – Cells were well distributed and encapsulated. 	1.5 × 2 cm. comp. mod. 10.3 kPa decreased to 2.4 kPa @ d14. Remained intact for 14 d	[74]
HUVECs + hBMSCs	GelMA + n-silicate + VEGF (gradient)	Extr-based direct-writing	UV	<ul style="list-style-type: none"> – Support cell survival and proliferation. – High structural stability @ 21 d. – Capillary formation. – Synergy between EC and MSC. – MSC in inner fibers differentiate to vascular myocytes. 	Problem with maintaining structure @21 d. Gradient, vascular channels.	[9]
mBMSC D1 cell line	Col + nHAp discs	LAB: NIR pulsed laser beam		<ul style="list-style-type: none"> – Significant bone formation in central type (mouse calvarial defects). – 2 mo postop, homogeneous bone regeneration 	Central 2 mm. Ring (2 mm inner and 3 mm outer f)	[13]
MC3T3-E1	Chitosan + n-HAp, Alg + n-HAp	Extr (Fab@ Home 3)	Thermal 32–37 °C for chitosan CaSO ₄ then CaCl ₂ for Alg	<ul style="list-style-type: none"> – Viab. ≈89–93% @d3 and 90–95% @d9. – Higher cell growth on HAp scaffold and on chitosan than in Alg constructs. – Higher proliferation on chitosan and chitosan-HAp. Increased with time in chitosan-nHAp. – Higher ECM production and mineralization on nHAp gels. 	Chitosan hydrogels had higher elastic mod than Alg.	[67]
Porcine fat tissue SVF-derived cells	Me-HA, Me-Gel or HA alone or with PCL/HAp	2 head Extr bioprinter (bioplotter = >pneumatic)	UV	Improved in vitro and in vivo vascularization and no neg effect on osteogenesis.	8 mm ø, 2 mm thick cylinder-like	[70]

methacryloyl (GelMA) is another example of modified natural polymer, which is becoming an important biomaterial in 3D bioprinting.^[82,83] GelMA can be chemically crosslinked with light to improve its stability under physiological conditions.^[18] GelMA was also combined with MeHA (GelMA/MeHA) and used in printing inks. The addition of MeHA was found to improve the mechanical properties of printed 3D constructs.^[18] However, with more complex materials, the challenge is to preserve important physical and chemical properties of the biomaterial which are necessary for processing and for the function of the resulting constructs. In addition, synthetic polymers such as Poloxamer 407 (Pluronic F-127),^[25] poly(ethylene glycol) (PEG),^[84,85] and PEG dimethacrylate (PEGDMA) were investigated for bone bioprinting^[15] with varying results (Table 2).

3.3. Bioink Crosslinking

The structural stability of a printed material can be improved by gelation using postprinting crosslinking techniques.^[52] **Figure 6** illustrates various crosslinking approaches which can be either chemical, physical, or both.^[53] Chemical crosslinking methods include the use of tyrosinase for gelatin,^[52] tannic acid for collagen,^[54] and factor XIII (fibrin stabilizing factor), which is activated by thrombin for fibrinogen. Methanol, glutaraldehyde, and EDC-NHS,^[58] which are commonly used agents for crosslinking, are not suitable for use after bioprinting, because they may affect cell viability and functional integrity of bioprinted constructs.^[52] Chemical crosslinking can also be achieved, e.g., by the use of UV light for GelMA.^[9,59] Physical crosslinking approaches include thermal gelation for collagen and sonication

for silk fibroin,^[52] and ionic gelation using calcium,^[29,56] barium or strontium^[57] for alginate. Many of these methods can affect cell viability,^[60] and thus, their use and exposure time should be carefully adjusted. UV is usually used with a photoinitiator, and one study that compared the effect of five photoinitiator agents on cell viability, showed that Irgacure 2959 and VA-086 are the most promising ones.^[61] While Irgacure 2959 radical exhibits cytotoxicity, VA-086 was associated with ≈90% viability. In addition to effect on cell viability, the choice of crosslinking method will influence also stability of the resulting structure of the construct. For example, the diameter and architecture of the resulting fibers may differ, depending on gelation rate, and used crosslinking technique and time. For example, a slow-gelling agarose may result in the formation of broad fibers, which tend to fuse, affecting the stacking of layers in the resulting scaffold.^[62] All these factors have to be balanced to produce bioconstructs having appropriate stability, appropriate function and clinically relevant size.

3.4. Additives to Bioinks to Improve Physiochemical and Biological Properties

To engineer the mechanical, rheological, and biological properties of bioinks, a broad range of materials have been used. The main focus has been put on improving the mechanical resilience of printed bone constructs while enhancing the osteoconductive and osteoinductive properties. Common materials to increase the mechanical strength of bioprinted bone constructs encompass polymers, micro- and nanoparticles, and fibers. In addition, bioactive additives, such as hydroxyapatite (HAp) and

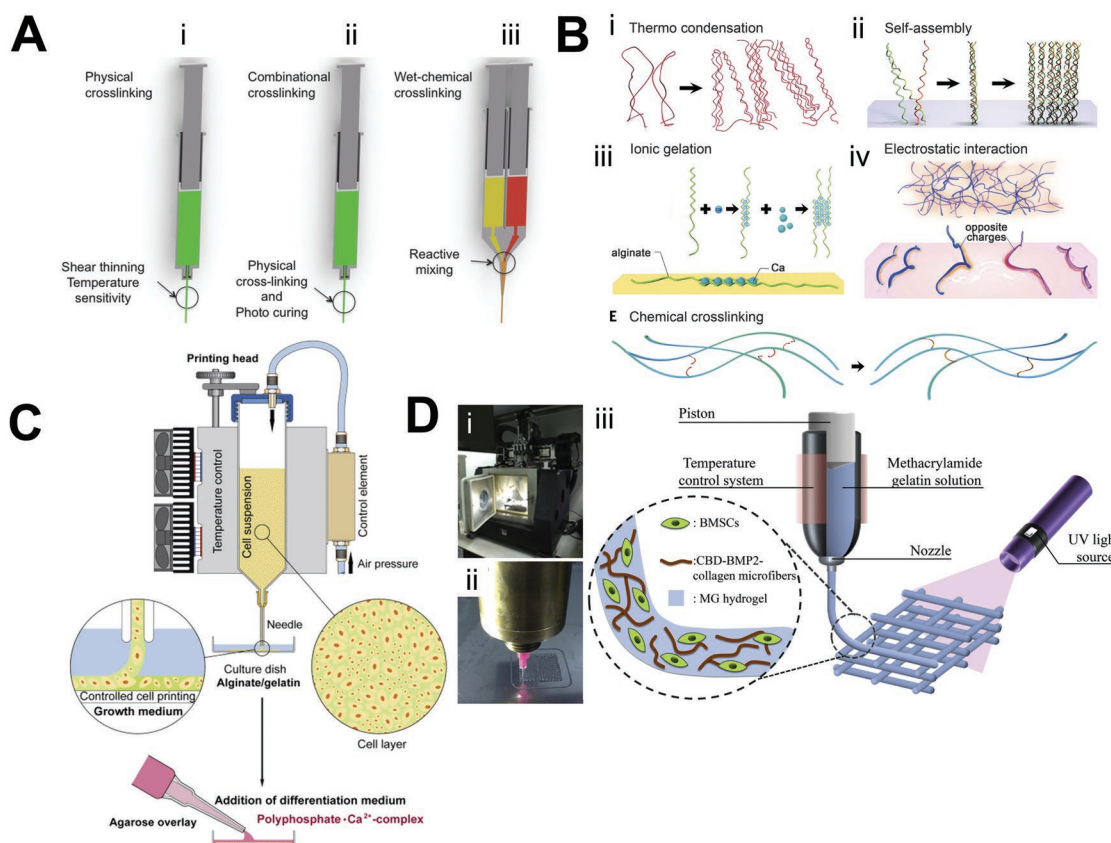


Figure 6. Crosslinking methods. A) Illustration of crosslinking methods: physical i,ii), combinatorial, and wet-chemical iii) for extrusion bioprinting. Reproduced with permission.^[171] Copyright 2013, Wiley-VCH. B) Methods of hydrogel crosslinking. Physical crosslinking methods i–iv) include thermally induced polymer-chain entanglement i), molecular self-assembly ii), ionic gelation iii), and electrostatic interaction iv). Chemical crosslinking v). Reproduced with permission.^[53] Copyright 2017, American Association for the Advancement of Science. C) Illustration showing 3D cell bioprinting of SaOS-2 cell-laden alginate/gelatin. The printed bioink passes through a CaCl_2 bath. This construct is then overlaid with an agarose layer containing osteogenic differentiation medium. Reproduced with permission.^[76] Copyright 2014, Elsevier. D) Illustration showing photo-crosslinking of the bioprinted construct. Reproduced with permission under the terms of the Creative Commons Attribution 3.0 license.^[73] Copyright 2015, the Authors. Published by IOP Publishing Group.

bone morphogenetic protein 2 (BMP-2) have secured a key role in imparting osteoconductivity and osteoinductivity, respectively, to 3D bioprinted bone constructs.

3.4.1. Reinforcement, Improving Mechanical Properties

Several strategies have been suggested to enhance the strength of hydrogel-based systems, such as the reinforcement of printed hydrogels with thermoplastic polymers^[86] or bioceramics.^[29,87] In one example, simultaneous deposition of hydrogels and reinforcing electrospun fibers was carried out (Figure 7). In addition to nanofibers,^[88,89] nanoparticles,^[87] microparticles,^[69] microcarriers,^[90] and struts^[65] have been used to provide mechanical support or improve the strength of bioprinted constructs. Furthermore, crosslinking of bioprinted constructs by UV-rays and chemical agents does not only improve their mechanical properties but it also increases the stiffness, longevity as well as thermal stability of 3D printed constructs.

In one study, poly(lactide-co-glycolide)-PEG (PLGA-PEG) microparticles were used to provide strength advantages

to BMSC-laden carboxymethyl cellulose (CMC). Values in the range matching those of cancellous bone were achieved (yield stress of 1.22–1.15 MPa and Young's modulus of 54.4–57.3 MPa).^[69] However, a high microparticle content was associated with reduced cell viability. This is probably related to increased stress exerted on the cells during extrusion, as a result of reduced amount of lubricant (viscous CMC). Further work to attain balance between cytocompatibility and PLGA particle concentration (with improved mechanical properties) should be conducted.^[69] In another study, HAp nanoparticles were used and nanoparticle concentration of 0.5 mg mL⁻¹ was found to be optimal for achieving the highest strength and bioactivity in GelMA scaffolds thus, making them promising for use in low load-bearing bones.^[87] Furthermore, the compression modulus was shown to be improved by using PLA microparticles (microcarriers) in MSC-laden gelatin methacrylamide-gellan gum bioink.^[90] Mechanical support of 3D printed hydrogel constructs can also be obtained by externally applied PCL reinforcement and Pluronic F127 temporary support.^[25] In future, strategies that combine cellular (hydrogel-based) and acellular strong 3D printed constructs can be developed.

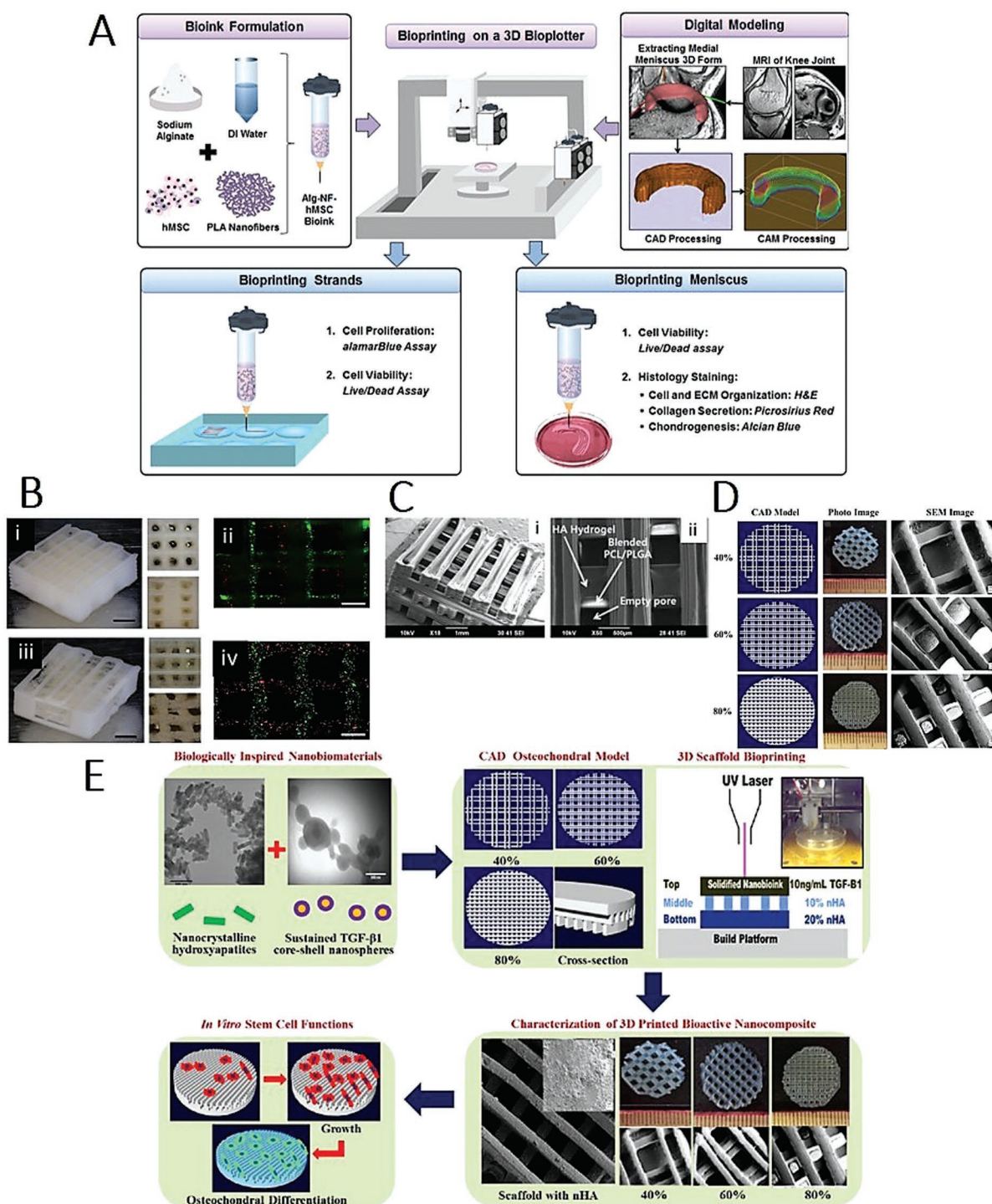


Figure 7. Construct reinforcement. A) Combining nanofibers. Bioprinting of a polylactide (PLA) nanofiber-alginate hydrogel bioink with encapsulated human adipose-derived stem cells (hASC). Reproduced with permission.^[89] Copyright 2016, American Chemical Society. B) 2D/3D patterning conducted by using the ITOP system. i–iv) Basic types of 3D patterning include type I i–iii), and type II iv–vi) patterns. Two 3D patterning types were produced, and they included cell-A (red), cell-B (blue), and PCL (green), by the integrated organ printing i,iv); photographs ii,v) and fluorescent image iii,vi) of the 3D printed patterns. Reproduced with permission.^[25] Copyright 2016, Nature Publishing Group. C) Combined deposition of PCL/PLGA and HA hydrogels. Scanning electron microscopic (SEM) images of printed PCL/PLGA construct with infused HA hydrogel i,ii). Reproduced with permission.^[86] Copyright 2011, IOP Publishing. D) CAD models, optical, and SEM images of a hydrogel construct with varying in-fill densities. Reproduced with permission.^[49] Copyright 2015, The Royal Society of Chemistry. E) Flow chart of SL-printed biomimetic nanocomposite osteochondral construct. Nanomaterials for differentiation of specific hMSCs into osteogenic (nHA) and chondrogenic (TGF- β 1 loaded PLGA nanospheres) cells. CAD model of porous construct design and composition. 3D printed bioactive constructs via table-top SLG and in vitro hMSC studies. Reproduced with permission.^[49] Copyright 2015, The Royal Society of Chemistry.

3.4.2. Osteoconductive Elements

To enhance bone formation, various osteoconductive elements have been added to bioinks. Studies have reported adding HAp,^[11,13,15,67,70,74,77] TCP^[25,29,54,91,92] or other osteoconductive materials^[9,56,64,66,75,76,92] (Table 2). HAp is a major component of the bone,^[93] and hence, it is used in bone 3D bioprinting. Even with synthetic polymers such as PEGDMA, adding HAp to hMSC-laden constructs was associated with increased osteogenesis.^[15] In addition, the use of TCP was explored, and results showed that α -TCP can provide osteoconductivity and has higher solubility than β -TCP does.^[94] In aqueous medium under neutral pH, α -TCP forms calcium-deficient HAp.^[29] α -TCP paste-extruding deposition was thus, used to develop the core of constructs having a printed shell made of preosteoblast (MC3T3-E1) -laden alginate hydrogel.^[29]

Other materials, such as polyP·Ca²⁺-complexes, orthosilicate (silica), and biosilica were used in alginate/gelatin hydrogels and bioprinted with bioactive glass (BaG) and SaOS-2 cells.^[75] It was found that adding BaG can increase bioprinted SaOS-2 cell proliferation and mineralization. In contrast, a study that used BaG nanoparticles with PEGDMA gels reported that cell viability was worse with BaG (63.80 ± 7.54%) than with HAp nanoparticles (86.62 ± 6.02%), possibly due to higher cytotoxicity associated with BaG.^[15] In earlier studies, it was found that concentrations ≥ 0.2 mg mL⁻¹ of BaG nanopowder were more cytotoxic than micropowder.^[95] Thus, the concentrations of used nano-BaG have to be carefully adjusted to gain osteoconductivity advantage and avoid cytotoxicity, especially when BaG is used alone. In another study, it was shown that adding HAp to alginate and chitosan hydrogels was associated with better mineralization after 21 days in culture.^[67] In addition to the importance of possessing osteoconductivity, the porosity (%), size, levels, and interconnectivity) of the resulting scaffold also matters. It was demonstrated that osteogenic differentiation is higher in porous BMSC-laden calcium phosphate (CP)-particle-containing alginate than in nonporous constructs.^[56]

3.4.3. Osteoinductivity

For osteoinductivity, growth factors are usually used. The two most commonly used growth factors in bone bioprinting studies are BMP-2 and vascular endothelial growth factor (VEGF) because of their efficiency in producing vascularized bone constructs.^[1] BMP-2 can be used as a protein or a polynucleotide (DNA). For example, BMP-2 plasmids that were used in BMSC-laden 3D bioprinted CP-particle-containing alginate constructs^[56] led to induced alkaline phosphatase (ALP) activity and osteocalcin expression. However, although BMP-2 protein production was seen during the first week of culture, no bone formation was observed in the constructs implanted in the subcutis of mice for 6-weeks. BMP-2 was two-dimensionally (2D) printed onto acellular dermal matrix (ADM) which was used for the treatment of experimental 5 mm diameter parietal bone defects in mice. Bone formation covered 66.5% of the BMP-2 printed area of ADM when it was facing the dura (the source of cells) and only on areas of the discs that were printed with BMP-2 (spatial specificity).^[96] Similar results were observed

with 3D-printed BMP-2 patterns on DermaMatrix human allograft scaffolds, where C2C12 progenitors were found to differentiate into osteogenic cells in BMP-2 patterns, in a dose-dependent manner.^[97]

It is important to develop strategies for drug release that can be controlled in spatial and temporal fashion and in a graduated system.^[98] In recent research, bioprinted systems that integrate a gradient drug releasing system were developed.^[9] An interesting strategy involved the use of a 3D printing system to develop a sequential drug release from an alginate shell and a PLGA core, and it proved to be nontoxic to bone-marrow-derived mesenchymal stem cells (BMSCs)^[99] (Figure 5B). Because osteogenesis and angiogenesis are well synchronized, a smart biomimetic growth factor-releasing nanocoating was developed in which electrostatically assembled recombinant human BMP-2 (rhBMP-2) and recombinant human VEGF (rhVEGF) were released from the nanocoating by the effect of metalloproteinase 2 (MMP2). When MMP2 degrades the gelatin, the growth factors are released. ALP activity in MSCs rose more rapidly and was sustained for longer time in the MMP-triggered BMP-2 release system.^[1] Concomitantly, it is important to have good control over the release of VEGF because excess VEGF may lead to inhibition of osteogenesis.^[100]

It was observed that silicate nanoparticles included in bioprinted GelMA can induce hMSC differentiation in cultured bioprinted constructs. The degree of mineralization was dependent on the amount of silicate nanoparticles, with the greatest mineralization was observed with the concentration of 100 µg mL⁻¹.^[9] Sodium ions (Na⁺), magnesium ions (Mg²⁺), silicic acid (Si(OH)₄), and lithium (Li) resulting from synthetic silicate dissociation in aqueous media may induce osteogenic cellular responses.^[101] The release of silicon oxide and magnesium oxide from 3D-printed TCP scaffolds was shown to accelerate bone formation and increase angiogenesis in rat's femoral bone.^[102] Although, hBMSCs osteogenic differentiation in 3D bioprinted methacrylated high-molecular weight HA (MeHA) occurred without the addition of other osteogenic stimuli, the addition of BMP-2 resulted in more mineralization occurring in the hydrogels.^[71]

3.5. Cells

Selecting the appropriate cell types for bone bioprinting is critical for the success of fabricated 3D bioprinted constructs. To mimic native bone tissue, 3D bioprinted constructs should ideally include different cell types, such as osteogenic and angiogenic cells. To date, cells used for bone bioprinting included various osteogenic cell types.^[9,15,18,52,55,62,64,66,68–71,73] For angiogenesis, endothelial cells (ECs)^[9,30,55] or endothelial progenitor cells (EPCs),^[66] have been used (Table 2). Although BMSCs are widely used for bone engineering, human turbinate MSCs (hTMSCs) were also explored for 3D bone bioprinting.^[52] They can be obtained from discarded tissue following inferior turbinate removal procedure carried out for the treatment of nasal obstruction.^[103] The cells have a very high yield (30 ± 1.2-fold increase in nasal septal progenitors relative to BMSCs),^[104] and they can differentiate into multiple lineages.^[103] In addition, donor age and passage have no significant effect on their

differentiation characteristics [unlike BMSCs or adipose tissue-derived mesenchymal stem cells (aMSCs)].^[103]

Moreover, MSCs were recently derived from induced pluripotent stem cells (hiPSCs) and they can be used to circumvent the problem of limited number of initial autologous MSCs that can be obtained from conventional sources such as bone marrow. Furthermore, during the reprogramming process, iPSC-derived MSCs (iMSCs) become also rejuvenated and show better survival, proliferation and differentiation capacity.^[105] These advances in stem cell technology may provide alternative cell sources for personalized bone bioprinting in future.

In bioprinting, cells can be employed as individually encapsulated or as dispersed cells in hydrogel precursor, or they can be used in microcarriers and cell aggregates (spheroids).^[42] Single-cell encapsulation^[41] for bioprinting^[39] is opening new possibilities to build tissues/organs block-by-block (modular tissue engineering), and to add various molecules, drugs, and markers into the resulting constructs.

3.6. Role of the Microenvironment

In early cell differentiation, soluble factors can be more important, but at later stages, other factors such as matrix elasticity become also important. For example, it was shown that MSCs are extremely sensitive to tissue-level elasticity, and it has been suggested that rigid matrices may be associated with osteogenic differentiation, whereas stiff matrices with myogenesis, and soft matrices with neurological cell differentiation.^[106] In bioprinted scaffolds, increased calcium deposition was found to be associated with stiff crosslinked nanocoated surfaces.^[1] There was, however, a different observation in a study by Campos et al.,^[72] who used collagen type I-agarose hydrogel blends with hMSCs for bone 3D bioprinting. More osteogenic differentiation of MSC was observed with less stiff blends. Further studies are needed to clarify this issue and have definitive answers.

In 3D printed constructs, cell guidance can be influenced by both chemical and physical cues,^[107] and it was shown that C2C12 cells can assume a position parallel to the orientation of polystyrene fibers that were coated with serum or fibrin. However, cells in regions of fibers printed with BMP-2 had also increased ALP expression.^[107] As a means of physical guidance, i.e., through cell adhesion, the use of arginyl-glycyl-aspartic acid (RGD), which is recognized by cellular integrins, has been explored. Engineered human-safe RGD-phage nanofibers were combined with chitosan and used in a 3D-printed ceramic (BCP, HAp/ β -TCP 80/20) scaffolds. When scaffolds were seeded with MSCs, they were found to induce osteogenesis and angiogenesis in rats' radial bone defects.^[92] Interestingly, RGD-phage was found to induce MSC osteogenic differentiation without the need for an osteogenic supplement.^[108]

In studies on the effect of electromagnetic field on stem cells, it was found that under specific conditions it leads to accelerated tissue formation.^[109] It was also noted that cell movement and migration can be guided by the application of small electric fields, which can improve in vivo bone healing.^[110,111] The physicochemical and electrical properties of a biomaterial can also be manipulated to control cell behavior in the 3D printed

construct. For example, polylysine was used because it is positively charged and thus, can promote cell adhesion by enhancing electrostatic interactions with the negatively charged cell membrane.^[1] Because magnetic nanoparticles can stimulate tissue growth through the application of magnetic fields,^[112] PCL and PCL/iron oxide scaffolds having coaxial and bilayer structure were investigated, and it was found that hMSCs spread well and adhere better on magnetic nanoparticle/PCL scaffolds.^[113]

4. Bioprinted Bone Constructs

Relevant studies on bone bioprinting are summarized in Table 2. Integrated advances for the development of well-controlled bioinspired tissue constructs that precisely mimic the microstructure of bone tissue have been investigated^[9] (Figure 8).

4.1. Fabrication

It is important to note that reduced complexity of bioprinting fabrication can increase the potential for industrial production.^[68] However, certain degree of complexity is inevitable, and it is required for the fabrication of biomimetic tissues. As discussed above, to produce appropriate osteoconductive constructs, various materials need to be combined, and thus, modifications are required to adapt 3D bioprinters to print different biomaterials. In one stage approach, cells and ceramic containing hydrogels are used to print constructs. For example, SaOS-2 cell-laden BaG nanoparticle-containing alginate/gelatin hydrogel was used to 3D print constructs.^[75] In another approach, a two-step printing process was used for bioprinting cell-laden collagen coating onto an α -TCP/type-I collagen 3D printed core (Figure 9).^[54] With the use of a one-step PEG scaffold 3D bioprinting, crosslinking, conjugation of acrylated RGD and acrylated MMP sensitive peptides and encapsulation of hMSCs can also be achieved. Constructs were printed layer-by-layer and simultaneously photopolymerized. With simultaneous photopolymerization, cells were distributed evenly in the resulting 3D bioprinted constructs. The whole 3D bioprinting process for each construct took less than four minutes.^[68]

In addition, the use of microfluidic bioprinting was found to be useful for mixing of bioink constituents and for precise control over the resulting product morphology. For instance, the use of two inlet snake micromixing chips was found to achieve a homogeneous distribution of cells in printed microfibers. In one study, microfluidic microfiber bone bioprinting was achieved by using a hydrogel made of either alginate with a gelatin solution or alginate with a particulate urinary bladder matrix (UBM) and SaOS-2 cells.^[57] In another study, alginate fibers were bioprinted by using microfluidic channels containing CaCl_2 solution as a crosslinking agent, and the bioprinted fibers were pulled on a roller. The fiber size was initially determined by microchannel diameter and was further reduced by rolling, down to 1 μm in diameter.^[114]

Most recently, a vascularized osteon-like bone construct was engineered using extrusion-based bioprinting with the

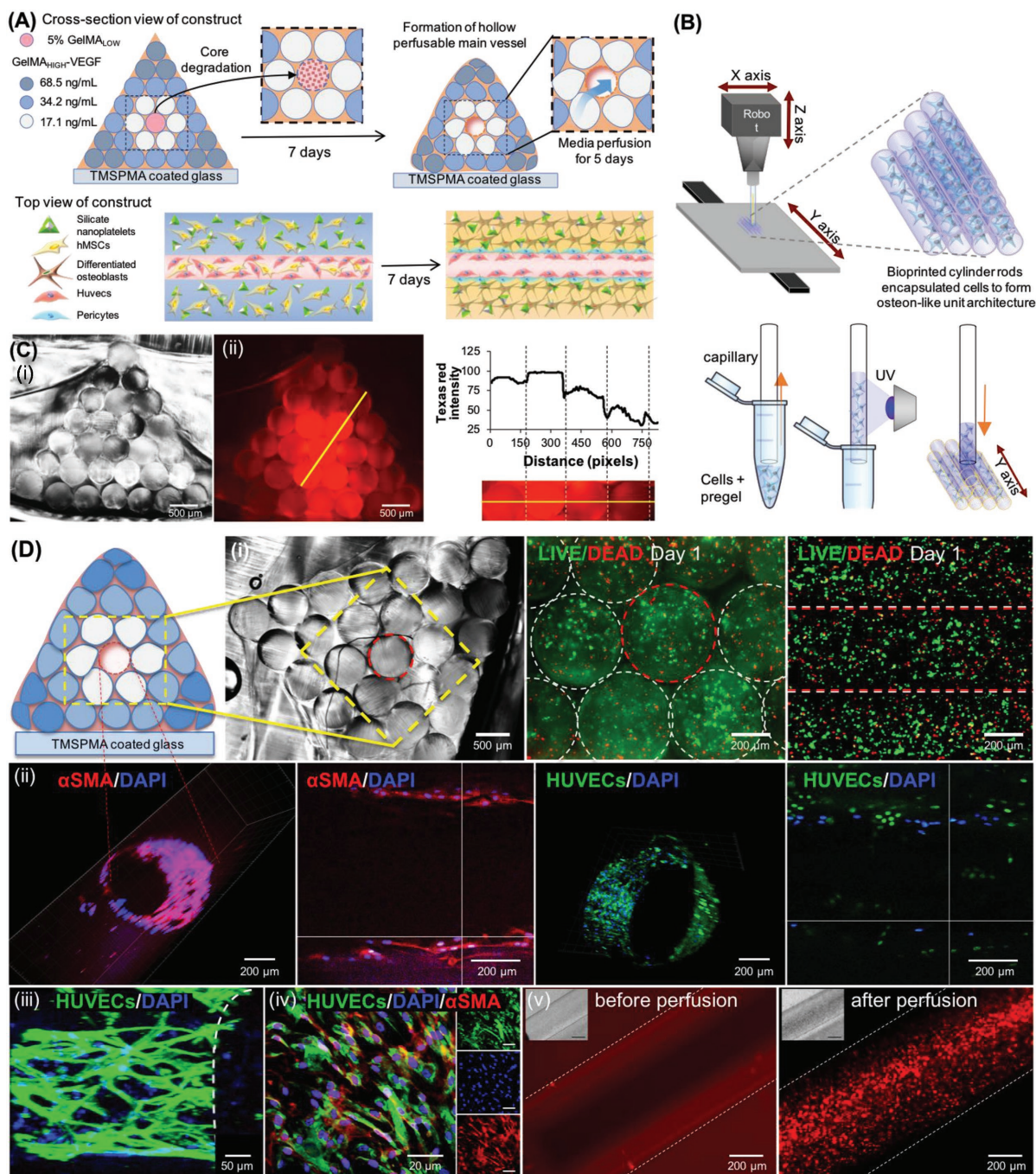


Figure 8. Development of biomimetic bone tissue construct. A) Schematic illustration of the bioprinting strategy used for building bone architecture. A perfusable HUVEC-lined vascular lumen was fabricated within the bioprinted construct by arranging individual VEGF-functionalized GelMA rods with varying mechanical strength. To induce osteogenic hMSC differentiation, the three outer layers of the cylinders were loaded with silicate nanoparticles. The three outer layers of the cylindrical hydrogels also had VEGF covalently conjugated to them. B) Schematic illustration of the 3D printing process of independent cell-laden cylinders employing an automated bioprinter. C) Cross-sectional image of the bioprinted construct (i) and chemical conjugation of a gradient (Texas Red) onto $-\text{COOH}$ modified GelMA fibers (ii). The intensity of fluorescence is directly proportional to the amount of conjugated dye. D) Formation of HUVEC/hMSC-lined perfusable lumen in the construct. The construct contains GFP-labeled HUVECs (GFPHUVECs) and hMSCs, which were cocultured for seven days, then perfused for five days. i) Cross-sectional view of the construct. Cross- and top-view of the construct showing encapsulated cells stained as Live or Dead inside the construct. ii) HUVEC-lined lumen within the construct. Cross- and top-sectioned confocal micrographs of the central vessel within the construct, which was stained with DAPI and α -SMA on day 12 post culture. Encapsulated ECs lined the vascular walls (green), and pericytes differentiated from hMSCs (red). iii) EC lining of the central channel. iv) Immunostaining of ECs and α -SMA-expressing hMSCs in the inner part of the lumen. v) Vascular lumen network perfused with a fluorescence microbead suspension at day 7 postculture. Images of the 3D hydrogel construct before and after microbead perfusion through the lumen. Reproduced with permission.^[9] Copyright 2017, Wiley-VCH.

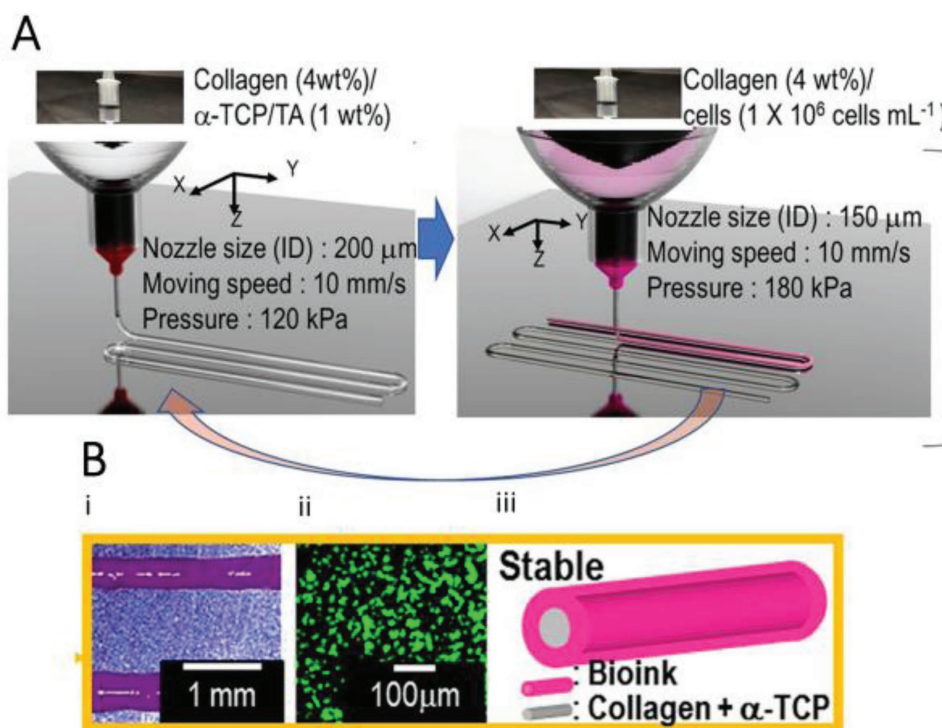


Figure 9. A two-step printing process. A) Illustration of a two-step printing process used for bioprinting preosteoblast (MC3T3-E1)-laden collagen coating onto α -TCP/type-I collagen 3D printed core. B) Images showing cell-laden collagen coating i), and in situ staining showing live (green) and dead (red) cells ii) following printing with the cell-laden collagen. iii) Illustration of cell-laden collagen coating of TCP/collagen core. Reproduced with permission under the terms of the Creative Commons Attribution 4.0 International License.^[54] Copyright 2017, the Authors. Published by Nature Publishing Group.

coculture of ECs and hMSCs in a GelMA hydrogel. To combine two types of tissues in one construct, cylinder-shape cell-laden hydrogels with different compositions were bioprinted. A higher mechanical stiffness on one side of the construct and encapsulated silica nanoplatelets were used to induce osteogenesis, and chemically conjugated VEGF was used to stimulate angiogenesis. The 3D bioprinted constructs were stable for 21 days in vitro. After seven days, a perfusable vascular channel developed in the middle of the bioprinted construct. Perfusion enhanced the mineralization of bone-like matrix and supported the maturation of the construct. However, there were difficulties with maintaining the structural stability of the construct after 21 days in culture due to the degradation of the GelMA gel.^[9]

4.2. Construct Physical Properties

4.2.1. Size and Porosity

The size of 3D bioprinted bone constructs that were produced so far ranges from 2 to 3 mm, using laser-assisted^[13] technique, to 1–2 cm, using microextrusion bioprinting.^[64,74] To the best of our knowledge, the largest construct so far was produced by Kang et al. (3.6 cm \times 3.0 cm) and it was thought to be appropriate for mandibular bone reconstruction.^[25] Constructs are usually in the form of porous structures comprising several layers.^[74] Sawkins et al.^[69] produced a

construct that has a porosity of 10.8–12.4% and mean pore size of 65.3–76.6 μ m. McBeth et al. generated constructs with larger pore size of 400 \times 400 μ m through the extrusion of a printed GelMA lattice coated on a titanium substrate; this construct could be used to improve implant osteointegration by triggering mineral deposition of MG63 lines and primary human osteoblasts.^[59] An ideal construct for bone engineering should have high porosity and interconnected channels and pores,^[73] with pore size of 200–400 μ m to promote in vivo tissue growth.^[115–118]

4.2.2. Degradation and Structural Stability

For constructs to be suitable for the engineering of bone tissue, they need to have reliable structural stability. Controllable construct biodegradation is particularly important. For example, it was reported that 3D-printed cell-laden alginate-PVA-HAP constructs remain intact for 14 days in cell culture media,^[74] and 3D bioprinted BMSC-laden TCP-containing alginate constructs degrade completely in six weeks.^[56] For GelMA, it was found that 50% of the 3D-printed lattice degrades on day 4, with 80% of GelMA degrades on day 18 in type II collagenase solution. It is important to choose an appropriate UV exposure time to allow GelMA constructs to sustain their structure beyond 3–4 weeks in vitro. GelMA tends to retain its structure for four weeks in culture media.^[59] Cell-laden GelMA rods were found to degrade to a large extent due to cell-secreted enzymes,

and they barely maintained their bioprinted structure by 21 days.^[9] Cell-laden silk fibroin gelatin constructs crosslinked with sonication were also found to be unstable after 21 days. HA, when modified with methacrylic anhydride and photopolymerized into networks, is an excellent bioink because it can resist degradation from less than 1 day to almost 38 days. It also maintains its mechanical stability and biocompatibility.^[80] It was observed that any shape can be fabricated with an HA network composition of $\geq 2\%$ (w/v) (**Figure 10B**). In the future, programmed hydrogels with controlled tunable degradation profiles can be produced to provide personalized custom-made 3D constructs.^[119]

4.2.3. Mechanical Properties

The initial strength and the retention thereof in 3D-bioprinted bone constructs in aqueous media are also important aspects which need to be defined. 3D bioprinted constructs engineered by using natural hydrogels have a compression modulus (usually below 5 kPa) lower than that of synthetic polymer constructs (such as PEGDMA coprinted with HA, which can have a strength of 358 kPa).^[15] Alginate, for instance, loses much of its strength ($\approx 40\%$) after nine days in culture.^[120] Although there has been some success in building a gradient system and microchannels into a 3D-bioprinted bone constructs with a delicate biomimic structure,^[9] mechanical stability was lost after 21 days in culture. An SaOS-2 cell-laden gelatin-functionalized alginate hydrogel that was bioprinted and then overlaid with polyP·Ca²⁺ lost its mechanical stability

after five days in culture. When incubated for six days or longer, the cylinder-shaped constructs disintegrated.^[76] Some cell-laden 3D-printed hydrogel constructs (alginate, PVA and HAp) had compression moduli of 10.3 kPa, but decreased to 2.4 kPa over 14 days in culture.^[74] Cell-laden collagen-coated TCP-collagen scaffolds had an elastic modulus of 0.55 ± 0.10 MPa^[54] which is lower than that of the trabecular bone (20–52 MPa in bone having a density of $0.09\text{--}0.75\text{ g cm}^{-2}$).^[121] Three-dimensionally bioprinted BaG and HAp particle-containing scaffolds were found to be softer than PRG gel-only ones. However, by 21 days, they recovered their stiffness, possibly due to ECM production by loaded MSCs differentiating into osteogenic cells.^[15] Alternatively, core-shell constructs (α -TCP core and cell-laden alginate shell) exhibited good compression strength (3.2 MPa) and structural preservation for 35 days in vitro.^[29] With the current limitation in strength retention, it is very difficult to have mechanically reliable constructs that can be used in clinical applications. Thus, there is a need to develop constructs with higher initial and retained strength properties.

4.3. Cell Function

4.3.1. Cell Viability

Cell viability represents an important measure for assessing the outcome of the 3D bioprinting process. It may be affected by different factors such as cell type, biomaterial type and properties, bioprinting process, and crosslinking method and agents.

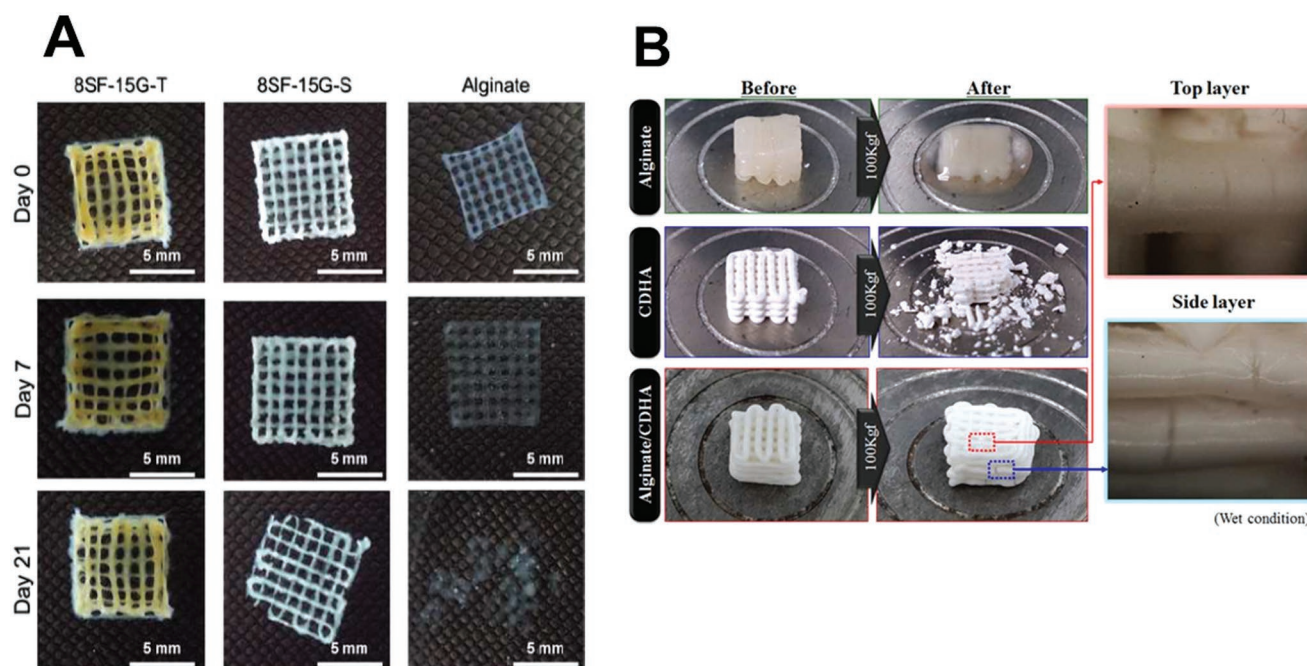


Figure 10. Construct strength and stability. A) Images showing long-term stability of 8% w/v silk-fibroin and 15 wt% of gelatin crosslinked with tyrosine (8SF-15G-T) or crosslinked with sonication (8SF-15G-S), and alginate (control) constructs in culture media. Reproduced from Das et al.^[52] with permission from Elsevier. B) Images showing the results of compression tests compared to their appearance before testing. Constructs made of alginate, calcium-deficient hydroxyl apatite (CDHA), and CDHA/alginate core/shell scaffolds are shown. Reproduced with permission.^[29] Copyright 2016, The Royal Society of Chemistry.

The choice of cell type is important to the function of the 3D bioprinted construct and its resemblance to native tissue. There are cell types which can be more sensitive than others when exposed to various stresses and insults during the printing process. This issue can be a subject of interesting future studies. Different biomaterials were successfully used for 3D bioprinting of bone tissue including natural biomaterials such as alginate, synthetic biomaterials such as PEGDMA or modified natural biomaterials such as GelMA (Table 2). An important property of a biomaterial that may influence cell viability is its viscosity. Generally, highly viscous biomaterials provide structural support to printed constructs, whereas low-viscosity materials are better for maintaining cell viability and function.

In early bioprinting studies, Poloxamer 407 (Lutrol) was used in bioinks and it was associated with only 4% cell viability at the 3rd postprinting day,^[62] and thus, alternative biomaterials were explored. Current reports on cell viability values have as high viability figures as $100 \pm 15\%$ immediately after bioprinting and $92 \pm 17\%$ after 24 h of incubation of osteoblast-like SaOS-2 cell laden alginate/gelatin hydrogels in vitro (bioprinted using a pneumatic microextrusion),^[76] and $>98\%$ after 21 days in culture of hMSC-laden thermoresponsive collagen type I-agarose blend hydrogels (bioprinted using inkjet-based 3D printing).^[72] Lower values of 64.4% viability after 21 days of culture were reported with hBMSCs laden MeHA hydrogels printed using pneumatic microextrusion.^[71] It was also noted that viability values are affected by time and medium, e.g., the average MC3T3 cell viability, which was assessed after bioprinting, in a blended hydrogel of alginate-PVA-HAP was 95.6%, and it was 77.5% after incubation in a calcium bath for 24 h.^[74] Moreover, in core-shell constructs (α -TCP core and cell-laden alginate shell), encapsulated MC3T3-E1 cell viability was more than 90% at 35 days.^[29] For comparison, at 4 h post-printing cell survival rate was $>91\%$ in preosteoblast (MC3T3-E1) cell laden collagen-coated α -TCP/type-I collagen,^[54] which does not seem to change much by time.

The type of method used for 3D bioprinting is also an important factor that affects viability. In earlier reports, it was also noted that microextrusion was associated with cell survival of lower than that of inkjet and laser-based bioprinting (40–86%) due to the extrusion pressure and shear stress^[24] (Table 1). However, recent studies reported cell viability of 97% with pressure extrusion printing as early as day 7,^[18] 64.4% with a piezoelectric inkjet at day 21,^[71] and 98% with a thermal inkjet at day 21 postprinting.^[72] When various goat BMSCs (gBMSCs)-laden hydrogels were bioprinted (using pneumatic extrusion) into fibers, there was no significant effect on cell survival due to the printing process.^[62] Using scaffold-free LAB bioprinting of hMSCs, no significant cell damage was observed and cells maintained their predefined structure for 21 days.^[48] Zhang et al.^[122] studied laser bioprinting-induced cell injury in mouse fibroblasts. They found that the minimum time needed for cells to complete apoptosis into late apoptotic cells was 4–5 h after printing. In microfluidic bioprinted SaOS-2-laden hydrogels with alginate/gelatin or alginate/particulate-UBM systems, cell survival was as high as 95%, and it was maintained for 14 days.^[57] In addition to the bioprinting process, crosslinkers, such as Irgacure 651 and Irgacure 2959 photoinitiators for UV

crosslinking, may induce cytotoxicity depending on their concentration and cell line.^[60,61] Among the photoinitiators, Irgacure 2959 has minimal toxicity against mammalian cells. In general, microextrusion-associated cell viability seems to have improved over time.^[24] However, when developing a new 3D bioprinting strategy, the biomaterial, crosslinking method, and other variables should be optimized to achieve the best cell viability outcomes.

4.3.2. Cell Proliferation

It is important to have cells proliferate in 3D bioprinted constructs, so they can develop into tissue-like structures. For example, in bioprinted collagen type I-agarose scaffolds, blends with higher collagen content and less stiffness were associated with more hMSCs cell spreading and branching.^[72] It was also noticed that the use of an overlaying polyP·Ca²⁺ complex on 3D bioprinted alginate/gelatin printed constructs can induce intense proliferation of SaOS-2 cells in the constructs.^[76] The biomaterial type and its composition can be detrimental to cell proliferation and subsequent tissue formation. Thus, the biomaterial should be carefully selected. In general, most of materials employed so far for bone 3D bioprinting have allowed for cell proliferation in the 3D bioprinted constructs (Table 2).

4.3.3. Cell Differentiation

Adult BMSCs can differentiate into various cell types, including osteogenic cells^[123] and it is important that such capability is preserved in bioprinted bone constructs. Many studies have shown that, following bioprinting of hMSCs, their mesenchymal phenotype can be preserved, and their osteogenic differentiation can be controlled by choosing the appropriate printing process, construct architecture, and regional bioactive factors.^[72] For instance, the osteogenic potential of hMSCs within an alginate/Matrigel was completely maintained following bioprinting.^[62] In another study, it was found that the indicators of osteogenic differentiation of encapsulated hMSCs at day 7 in PEG-peptide hydrogel were significantly higher than in PEG hydrogels.^[68] SaOS-2 osteogenic differentiation was also demonstrated to occur within seven days in bioprinted alginate/gelatin microfibers and alginate/particulate UBM scaffolds. Moreover, with other biomaterials such as MeHA, osteogenic differentiation of hBMSCs in bioprinted constructs occurred without the need for any additional osteogenic stimuli. Generally, adding BMP-2 results in more differentiation, as evidenced by mineralization of the matrix. The effect of mechanical properties of the biomaterial on cell fate was also discussed,^[124,125] and it was noted that increased biomaterial rigidity can be associated with more MSC osteogenic differentiation.^[71] MSC osteogenic differentiation was found to occur in photocrosslinked low-molecular weight HA.^[126] The importance of spatial cues was also demonstrated when a GelMA lattice (extrusion printed and UV crosslinked) and not films were found to trigger osteoblast mineralization (the clearest osteoblast differentiation indicator) in the MG63 line and in primary normal human osteoblasts (NHOst), in the absence of osteogenic media.^[59] Furthermore, the use of

osteoconductive materials such as HAp was found to improve osteogenic differentiation of preosteoblast cells in vitro.^[67] As regards the used crosslinking agent, microfibers that were crosslinked with strontium chloride were associated with more differentiation as compared to those crosslinked with either barium and calcium chloride.^[57] A significant increase in mineralization was observed with an additional layer of polyP-Ca²⁺-complex on a SaOS-2 cell-laden alginate/gelatin bioprinted hydrogel.^[76] It is evident that various physical and chemical factors can affect stem cell function in bone bioprinting, and when they are properly adjusted, osteogenic differentiation can be stimulated and enhanced.

4.4. In Vivo Bone Tissue Formation

Before implantation in vivo, keeping 3D bioprinted bone constructs in culture for some time is thought to improve the outcome. This time in culture will allow cells to proliferate, populate the channels/spaces in the scaffold and differentiate. In addition, one should consider possible cell division cycles and their impact on the function of the in vivo implantable graft.^[127]

There are only a few studies that have examined bone formation in bioprinted constructs in vivo. It has to be emphasized that in vivo implantation is the ultimate test for 3D constructs intended to use as tissue grafts. Although results may be encouraging in vitro, it is not always the case in vivo. For example, in a study that utilized BMP-2 plasmid DNA with BMSC-laden CP particle containing alginate bioprinted constructs, in vitro results showed BMP2 protein production during the first week of culture, but, in vivo there was insignificant bone formation during the six-week period of implantation in the subcutis of mice.^[56] In another study, Fedorovich et al. printed two different phases of gBMSCs and goat EPCs (gEPCs) in a Matrigel/alginate-BCP microparticle system. Bioprinted constructs were then implanted subcutaneously in mice. They were found to successfully integrate with the host tissue by forming microvessels in the endothelial cell progenitor-containing phase. This work demonstrated that multiple cell types can retain their function in a bioprinted material in vitro and produce ECM in vivo.^[66]

Kang et al. developed 3D-printed human amniotic fluid-derived stem cell (hAFSC) laden hydrogels (gelatin, fibrinogen, HA, and glycerol). Following bioprinting of fibrin, other supporting materials were washed out, and constructs were cultured for the following 15 days. Constructs were then implanted into experimental calvarial bone defects in rats, leading to new bone formation throughout the defects in five months.^[25] In bone environment, printed MSCs and collagen nano-HAp (nHAp) discs were used for the treatment of calvarial bone defects in mice and significant mature bone formation was observed two months postoperatively in defects where cells were printed onto the center of the discs. In comparison, no major bone formation was observed when cells were printed onto the periphery of the discs^[13] (Figure 11). These advances prove the principle, but nevertheless, more in vivo studies are needed to evaluate the integration and function of grafted bone into bone defects located in different types of bone, e.g. those in the long bones where challenges

and type of bone are different. This will pave the way for the development of custom-made constructs in the clinic, in future.^[17]

4.5. Functional Tissue Integration and Remodeling

One limitation of most engineered tissue constructs is that they rely on diffusion for their nutrient supply, and cells can survive this way at a distance of only 100–200 µm.^[128] Consequently, cell viability in the center of a construct will be severely compromised.^[129] The development of vascularized constructs will thus, be of great benefit for the healing of bone defects. Three-dimensional bioprinting holds great promise for producing structures that contain vascular networks for fluid exchange.^[45] It mimics the natural in vivo vasculature and represents a crucial step toward the engineering of functional bone tissue constructs.^[130] Toward this goal, successful examples include the work by Chen et al., who demonstrated the formation of a dense microvasculature in 3D constructs by using ECs and hMSCs encapsulated in a gelatin hydrogel.^[131]

It is important that angiogenesis precedes osteogenesis. Thus, when it is followed by the addition of osteogenic cells, osteoid deposition, bone fraction volume and anastomosis of formed vessels within the host can be improved.^[132] A system was developed whereby rhVEGF is released earlier from the top layer of the printed construct, followed by the release of rhBMP-2 from the deeper layer. The construct was cultured in EC growth medium for one week to form vascular networks, followed by culture in osteoinductive medium for an additional three weeks.^[1] It has to be noted that in vivo vascularization is a relatively slow process and it occurs at a rate of <1 mm per day of vessel growth within an implant.^[133] Additionally, coculture of osteogenic cells and ECs is required, however, factors such as hypoxia which can stimulate angiogenesis can inhibit osteogenesis.^[30,134] Thus, a biphasic bone construct was developed with highly organized vascular network^[30] (Figure 12). For the osteogenic phase, polydopamine-coated PLA fibers were printed by fused deposition modeling (FDM) extrusion, and they were seeded with MSCs. For the vascular phase, tubular structures were printed by using VEGF-conjugated GelMA hydrogels encapsulating MSCs and human umbilical vein endothelial cells (HUVECs) in a custom-designed bioreactor. A recent work has shown that short-term hypoxia can stimulate vascularization but does not affect osteogenesis either in vitro or in vivo.^[70]

It is worth noting that the “crosstalk” between osteoblasts and other cell types especially ECs as well as MSCs is important.^[135] It was found that when ECs were printed alone, they spread out randomly in a collagen hydrogel. In addition, the crosstalk between human osseous cell sheets and HUVECs in the presence of laser assisted bioprinting biopapers leads to the formation of human prevascularized cell-based osseous constructs that can be applied for autologous bone repair applications.^[136] However, when they were printed with MSCs, they remained in the printed lines, which again indicates the importance of coculture of the two cell types.^[137] In other attempts to enhance tissue survival and integration, vascularized

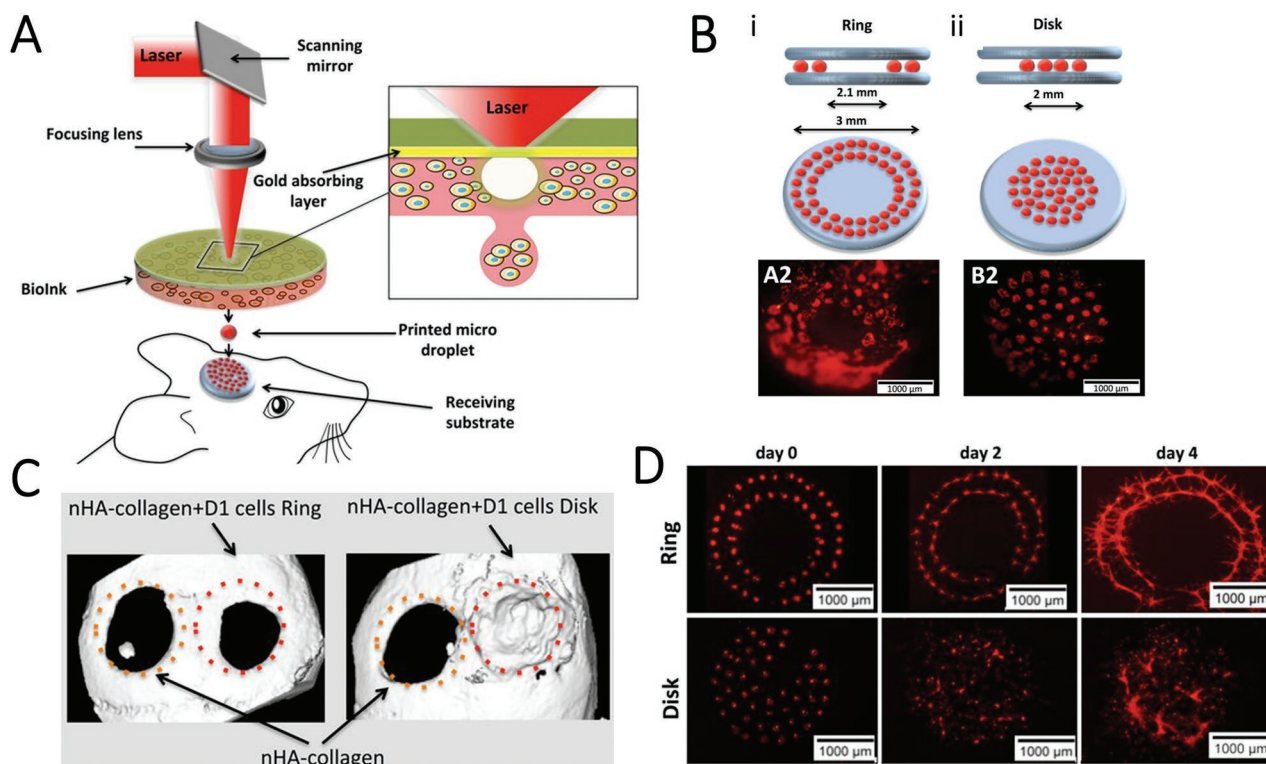


Figure 11. Osteoconductive discs and cell printing. Laser-assisted bioprinting used for printing cells on nHAp collagen discs that were used for the treatment of experimental calvarial defects in mice A) where cells were printed at the peripheral i) or central ii) areas of the discs B). Fluorescence images of peripherally A2) and centrally B2) printed tomato-positive cells inside defects, immediately after printing B). C) Microtomography (μ CT) reconstruction images, two months after surgery, showing that healing occurred in defects where cells were applied at the central area but occurred only at the periphery in cases where cells were applied peripherally. There was no bone formation in defects where no cells were applied (nHA collagen alone, defect in the left side). D) Fluorescence images of centrally and peripherally printed tomato-positive D1 cells at days 0, 2, and 4 after printing. Reproduced with permission.^[13] Copyright 2017, Nature Publishing Group.

heterogeneous tissue was developed by using ECs and fibroblasts^[138] (Figure 13). The importance of vascular and osteogenic cell coculture for osteogenesis has been demonstrated also in other earlier studies, when EPCs and gMSCs were cultured on Matrigel. EPCs were found to accelerate the osteogenic differentiation of MSCs, and in turn, MSCs supported EPC proliferation and stabilization of the vascular network.^[139] Although it depends on the environment, the best MSC/EC ratio needed for osteogenesis and angiogenesis was found to be 50:50.^[140,141]

In addition to vascularization of constructs, integration and anastomosis with the host vasculature after implantation are crucial. Bioprinted bone constructs were shown to form microvessels and to become integrated with the host tissue.^[66] Scherberich et al. seeded human adipose SVF cells into HAp scaffolds and cultured them within a 3D perfusion system.^[11] Subsequently, the construct was implanted into the subcutis of nude mice. After eight weeks, with perfused construct, there was a robust generation of bone and formation of blood vessels that were connected to the host vasculature. In control experiment (2D expanded cells), there was neither bone nor blood vessel formation. It was also found that media perfusion increased the length of microcapillaries which formed in the coculture of ECs and osteoblasts encapsulated in CP scaffolds.^[142]

Following implantation *in vivo*, bone needs to undergo remodeling, and it must be exposed to physiological loading gradually to become functional and integrate with the surrounding tissues. It should be noted that bone is generally a load-bearing tissue and that bone mineral density is load-dependent.^[143] Hence, loading of engineered bone constructs can significantly increase the synthesis of mineralized matrix, and may improve the development and maturation of engineered bone tissue. Obtaining functional bone is a multistage process that does not end at the time of implantation and vascularization. Continuous long-term follow-up to assess bone tissue development, remodeling and integration is thus, needed to perform in future *in vivo* studies.

5. Challenges and Future Perspectives

Despite advances made in bone bioprinting, several challenges face the production of clinically relevant, functional bone grafts.^[144] The main challenges comprise: 1) 3D bioprinted construct stability, 2) limited construct size, 3) vascularization,^[16,145] 4) loss of mechanical properties, 5) integration to native tissues, and 6) long-term function.^[16] Other related challenges include limited autologous cell supply, difference in the outcome of stem cell therapy between patients, and the risk of rejection and

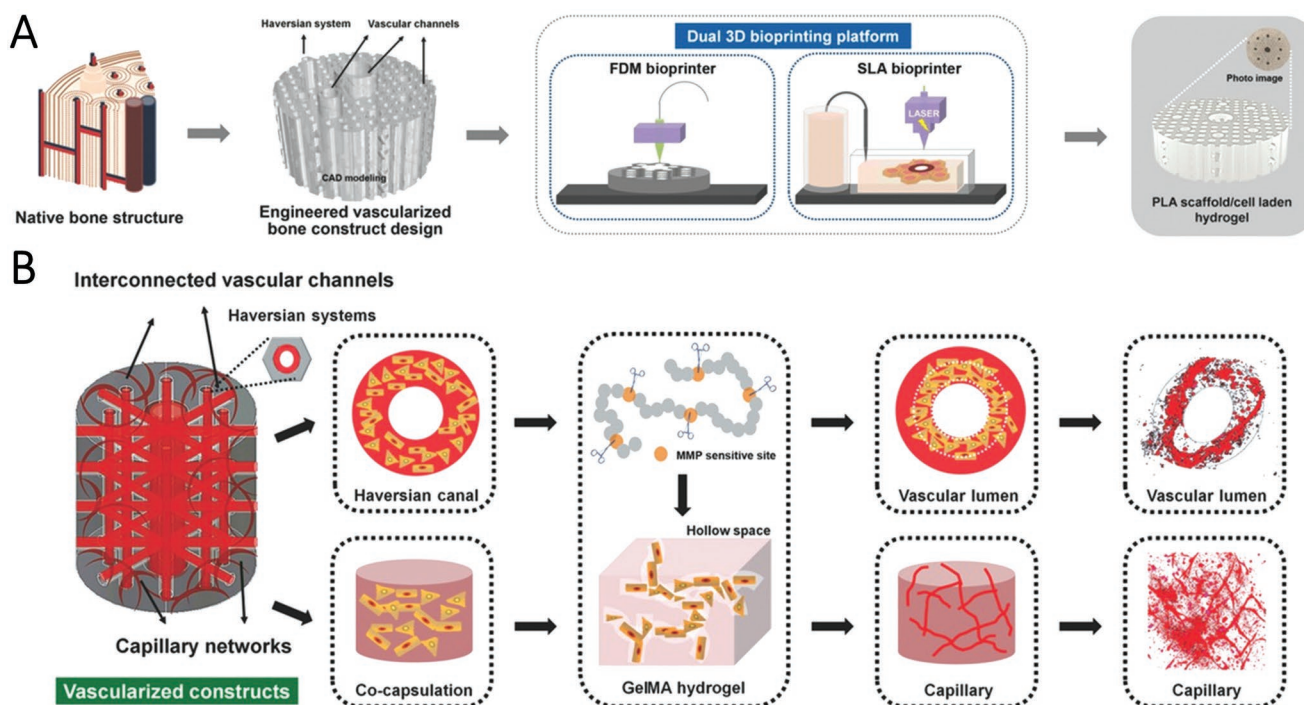


Figure 12. Biphasic bone construct with highly organized vascular network. A) Schematic illustration of vascularized biphasic construct fabrication involving biomimetic architectural design and hierarchical fabrication using dual 3D bioprinting. Schematic illustration of native bone structure, CAD modeling of a design of vascularized bone, schematic illustration of fused deposition modeling (FDM)/stereolithography (SLG) 3D bioprinting, and an image of a 3D vascularized bone construct. B) Schematic illustration of microstructural design of a vascularized construct employing matrix metalloproteinase (MMP) sensitive gelatin methacryloyl (GelMA) hydrogel. Vascular lumen and capillary network formation can be achieved in different regions while in culture. Reproduced with permission.^[30] Copyright 2016, Wiley-VCH.

disease transmission through allogeneic stem cell therapy.^[145] There are also issues related to applications, such as the complex CMF skeleton,^[146] concerns about the unregulated clinical use of stem cells,^[147] and regulatory approval aspects.^[148,149]

Acellular 3D-printed strong scaffolds can be combined with cellular 3D-bioprinted constructs to overcome the challenges of limited mechanical properties of cellular bioprinted bone constructs. Examples may include the use of hyperelastic bone biomaterial (90 wt% HAp and 10 wt% PCL or PLGA) along with

3D cellular constructs.^[150] New 3D printers allow the use of different materials to produce cellular and acellular constructs simultaneously. Using such printers, different components can be processed using different printing conditions (e.g., different temperature) without affecting each other.

Clinical translation will require the use of integrated bioprinting platforms that enable the utilization of multiple biomaterials to build biomimetic tissue constructs at a clinically relevant scale^[151] (Figure 1). Although there are differences

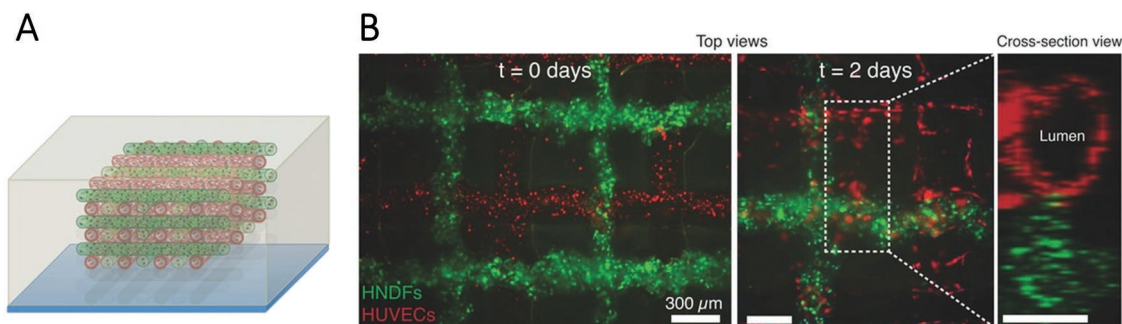


Figure 13. Development of vascularized tissue. A) Schematic view, and (B) fluorescence images i,ii) of an engineered vascularized tissue construct comprising different cell types, cultured for 0 i) and 2 ii) days, in which red and green filaments correspond to channels lined with red fluorescent protein-expressing human umbilical vein endothelial cells (RFP HUVECs) and green fluorescent protein-expressing human neonatal dermal fibroblast cells (GFP HNF) in a gelatin methacrylate (GelMA) ink. The cross-sectional view in (c) shows that ECs line the lumen of the 3D microvascular network. Reproduced with permission.^[138] Copyright 2014, Wiley-VCH.

between compact and trabecular bones, results have been obtained from various studies, can potentially be translated to other types. Nevertheless, studies using specialized models of either calvarial flat bones or long compact bone addressing specific and ultimate clinical indications are required. Once successful outcomes are obtained, the results can be translated to the clinic.^[17] In clinical application environment, the real challenges can be identified, and appropriate solutions devised. Clinical indications should be then precisely defined, when applying for regulatory body approvals.^[152] In the future, 3D bioprinting for clinical use can be achieved either by 3D printing in the therapy-providing centers or 3D printing at a central location that can deliver constructs to the relevant clinics.^[16] To enhance clinical applications of 3D bioprinting further, a handheld device was developed for in situ intraoperative printing.^[18] With the advances made in artificial intelligence and robotics, automatic robotic bioprinters may be realized in the future, and they may be controlled by an operating surgeon to achieve precise construct printing and implantation in the operating room.^[13,153]

Four-dimensional^[154–158] can be employed to produce 4D construct^[159] by adding cells to stimuli-responsive hydrogels^[160,161] that can render constructs dynamic and responsive to changes, e.g., in temperature,^[162] pH, and electrical or magnetic fields.^[163,164] As this opens up new possibilities, it will also bring about new challenges. In the resulting 4D constructs, cells should ideally have no adverse effects on biomaterial properties, and the biomaterial dynamics should not affect cell viability and function. The addition of reinforcing materials may also impart new properties to 3D bioprinted constructs, as may also be obtained with the use of shape memory materials.^[165]

Control of the micro- and macroenvironments by loading and using electromagnetic stimulation is one important area,^[166] that deserves further attention. Due to the piezoelectric nature of the bone, electromechanical mechanisms are involved in feedback that promotes osseous tissue adaptation and remodeling.^[151] For example, the application of small electric fields can be useful in improving in vivo bone healing^[110,111] and accelerating tissue formation.^[109] Conductive polymers, such as polypyrrole, polyaniline, and carbon nanotubes (CNTs), can be used to stimulate bone formation. These materials can be incorporated into bioprinted constructs to provide both structural stability and guided cell growth.^[82,151] To date, there are only few studies that have used 3D printing to produce piezoelectric scaffolds. The use of scaffolds containing CNTs demonstrated that osteoblast proliferation can be sustained with these PCL–CNT composites.^[167] Electrospun conductive PANi fibers can also be combined with conductive graphene-containing hydrogels in composites that can support osteogenic cell adhesion and proliferation.^[168] In future, such materials could be developed further to achieve functional bone 3D bioprinting.

Although multipotent stem cells and somatic cells have been used for bone bioprinting, it may also be possible to use iPSCs^[169] and iMSCs^[105] in 3D bioprinting to create tissue constructs that can be applied in treatment or can serve as models to study iPSCs and develop new drugs. The field is offering unprecedented opportunities to develop successful innovations for which the recruitment of several disciplines and convergence of science fields are required.

6. Conclusions

Bone 3D bioprinting has advanced recently, combining hydrogels, cells, and other osteoconductive and osteoinductive elements to produce viable bone tissue constructs. Moreover, mineralized structures with vascularized networks in vitro were produced. Although, there have been only few in vivo studies so far, they demonstrated the feasibility of the technology and potential for application in the treatment of bone defects. Bioprinted constructs need to have a stable structure, appropriate mechanical properties, and suitable function for sufficient time until complete healing and remodeling occurs. The size of produced constructs is currently, limited to a few centimeters at most. The challenge of producing clinically relevant large vascularized grafts and enabling their in vivo integration and remodeling remains to be addressed. To achieve success in this growing research area multidisciplinary approach and sustained funding are required.

Acknowledgements

The authors acknowledge funding from the National Institutes of Health (AR057837) and National Priority Research program, Part of Qatar Foundation, (NPRP9-144-03-021 and NPRP10-120-170211). All statements made herein are solely the responsibility of the authors. The authors also thank Mohammed Xohdy for drawing Figures 2 and 4.

Conflict of Interest

The authors declare no conflict of interest.

Keywords

3D bioprinting, bioinks, bone defects, tissue engineering

Received: August 28, 2018

Revised: November 26, 2018

Published online: February 8, 2019

- [1] H. Cui, W. Zhu, B. Holmes, L. G. Zhang, *Adv. Sci.* **2016**, 3, 1600058.
- [2] Y. Ikada, J. R. Soc., *Interface* **2006**, 3, 589.
- [3] J. J. Song, H. C. Ott, *Trends Mol. Med.* **2011**, 17, 424.
- [4] A. Oryan, S. Alidadi, A. Moshiri, N. Maffulli, *J. Orthop. Surgery Res.* **2014**, 9, 18.
- [5] A. R. Amini, C. T. Laurencin, S. P. Nukavarapu, *Crit. Rev. Biomed. Eng.* **2012**, 40, 363.
- [6] Y. Liu, D. Luo, T. Wang, *Small* **2016**, 12, 4611.
- [7] D. B. Burr, M. R. Allen, *Basic and Applied Bone Biology*, 1st ed., Academic Press, London, UK **2014**.
- [8] J. Rho, L. Kuhn-Spearing, P. Zioupos, *Med. Eng. Phys.* **1998**, 20, 92.
- [9] B. Byambaa, N. Annabi, K. Yue, G. Trujillo de Santiago, M. M. Alvarez, W. Jia, M. Kazemzadeh-Narbat, S. R. Shin, A. Tamayol, A. Khademhosseini, *Adv. Healthcare Mater.* **2017**, 6, 1700015.
- [10] B. Holmes, K. Bulusu, M. Plesniak, L. G. Zhang, *Nanotechnology* **2016**, 27, 064001.
- [11] A. Scherberich, R. Galli, C. Jaquiere, J. Farhadi, I. Martin, *Stem Cells* **2007**, 25, 1823.

- [12] M. Rodriguez-Salvador, R. M. Rio-Belver, G. Garechana-Anacabe, *PLoS One* **2017**, 12, e0180375.
- [13] V. Keriquel, H. Oliveira, M. Remy, S. Ziane, S. Delmond, B. Rousseau, S. Rey, S. Catros, J. Amedee, F. Guillemot, J. C. Fricain, *Sci. Rep.* **2017**, 7, 1778.
- [14] C. Arrigoni, M. Gilardi, S. Bersini, C. Candrian, M. Moretti, *Stem Cell Rev. Rep.* **2017**, 13, 407.
- [15] G. Gao, A. F. Schilling, T. Yonezawa, J. Wang, G. Dai, X. Cui, *Biotechnol. J.* **2014**, 9, 1304.
- [16] D. M. Gibbs, M. Vaezi, S. Yang, R. O. Oreffo, *Regener. Med.* **2014**, 9, 535.
- [17] N. Tellisi, N. Ashammakhi, F. Billi, O. Kaarela, *J. Craniofac. Surg.* **2018**.
- [18] C. D. O'Connell, C. Di Bella, F. Thompson, C. Augustine, S. Beirne, R. Cornock, C. J. Richards, J. Chung, S. Gambhir, Z. Yue, J. Bourke, B. Zhang, A. Taylor, A. Quigley, R. Kapsa, P. Choong, G. G. Wallace, *Biofabrication* **2016**, 8, 015019.
- [19] P. Datta, V. Ozbolat, B. Ayan, A. Dhawan, I. T. Ozbolat, *Biotechnol. Bioeng.* **2017**.
- [20] L. Ionov, *Adv. Healthcare Mater.* **2018**, 7, 1800412.
- [21] J. K. Placone, A. J. Engler, *Adv. Healthcare Mater.* **2018**, 7, 1701161.
- [22] J. M. Lee, W. Y. Yeong, *Adv. Healthcare Mater.* **2016**, 5, 2856.
- [23] S. Chawla, S. Midha, A. Sharma, S. Ghosh, *Adv. Healthcare Mater.* **2018**, 7, 1701204.
- [24] S. V. Murphy, A. Atala, *Nat. Biotechnol.* **2014**, 32, 773.
- [25] H. Kang, S. J. Lee, I. K. Ko, C. Kengla, J. J. Yoo, A. Atala, *Nat. Biotechnol.* **2016**, 34, 312.
- [26] N. A. Sears, D. R. Seshadri, P. S. Dhavalikar, E. Cosgriff-Hernandez, *Tissue Eng., Part B* **2016**, 22, 298.
- [27] I. T. Ozbolat, M. Hospodiuk, *Biomaterials* **2016**, 76, 321.
- [28] A. B. Dababneh, I. T. Ozbolat, *J. Manuf. Sci. Eng.* **2014**, 136, 061016.
- [29] N. Raja, H. Yun, *J. Mater. Chem. B* **2016**, 4, 4707.
- [30] H. Cui, W. Zhu, M. Nowicki, X. Zhou, A. Khademhosseini, L. G. Zhang, *Adv. Healthcare Mater.* **2016**, 5, 2174.
- [31] K. Arcaute, B. K. Mann, R. B. Wicker, *Ann. Biomed. Eng.* **2006**, 34, 1429.
- [32] N. Mehrban, G. Z. Teoh, M. A. Birchall, *Int. J. Bioprint.* **2016**, 2.
- [33] C. W. Hull, *U. S. Patent 4,575,330*, **1986**.
- [34] Y. Shanjani, C. C. Pan, L. Elomaa, Y. Yang, *Biofabrication* **2015**, 7, 045008.
- [35] X. Hou, Y. S. Zhang, G. Trujillo-de Santiago, M. M. Alvarez, J. Ribas, S. J. Jonas, P. S. Weiss, A. M. Andrews, J. Aizenberg, A. Khademhosseini, *Nat. Rev. Mater.* **2017**, 2, 17016.
- [36] T. J. Ober, D. Foresti, J. A. Lewis, *Proc. Natl. Acad. Sci. USA* **2015**, 112, 12293.
- [37] J. O. Hardin, T. J. Ober, A. D. Valentine, J. A. Lewis, *Adv. Mater.* **2015**, 27, 3279.
- [38] C. Colosi, S. R. Shin, V. Manoharan, S. Massa, M. Costantini, A. Barbetta, M. R. Dokmeci, M. Dentini, A. Khademhosseini, *Adv. Mater.* **2016**, 28, 677.
- [39] T. Kamperman, S. Henke, A. van den Berg, S. R. Shin, A. Tamayol, A. Khademhosseini, M. Karperien, J. Leijten, *Adv. Healthcare Mater.* **2017**, 6, 1600913.
- [40] A. S. Mao, J. W. Shin, S. Utech, H. Wang, O. Uzun, W. Li, M. Cooper, Y. Hu, L. Zhang, D. A. Weitz, D. J. Mooney, *Nat. Mater.* **2017**, 16, 236.
- [41] P. S. Lienemann, T. Rossow, A. S. Mao, Q. Vallmajo-Martin, M. Ehrbar, D. J. Mooney, *Lab Chip* **2017**, 17, 727.
- [42] C. Colosi, M. Costantini, A. Barbetta, M. Dentini, *3D Cell Culture: Methods and Protocols, Methods in Molecular Biology*, Vol. 1612 (Eds: Z. Koledova), Springer Science+Business Media LLC, New York, NY, USA **2017**, pp. 369–380, Ch. 26.
- [43] R. Chang, J. Nam, W. Sun, *Tissue Eng., Part A* **2008**, 14, 41.
- [44] C. Colosi, M. Costantini, R. Latini, S. Ciccirelli, A. Stampella, A. Barbetta, M. Massimi, L. Conti Devirgiliis, M. Dentini, *J. Mater. Chem. B* **2014**, 2, 6779.
- [45] G. Gao, X. Cui, *Biotechnol. Lett.* **2016**, 38, 203.
- [46] X. Cui, D. Dean, Z. M. Ruggeri, T. Boland, *Biotechnol. Bioeng.* **2010**, 106, 963.
- [47] S. Moon, S. K. Hasan, Y. S. Song, F. Xu, H. O. Keles, F. Manzur, S. Mikkilineni, J. W. Hong, J. Nagatomi, E. Haeggstrom, A. Khademhosseini, U. Demirci, *Tissue Eng., Part C* **2010**, 16, 157.
- [48] M. Gruene, A. Deiwick, L. Koch, S. Schlie, C. Unger, N. Hofmann, I. Bernemann, B. Glasmacher, B. Chichkov, *Tissue Eng., Part C* **2011**, 17, 79.
- [49] N. J. Castro, J. O'Brien, L. G. Zhang, *Nanoscale* **2015**, 7, 141.
- [50] R. Raman, B. Bhaduri, M. Mir, A. Shkumatov, M. K. Lee, G. Popescu, H. Kong, R. Bashir, *Adv. Healthcare Mater.* **2016**, 5, 610.
- [51] Z. Wang, Z. Tian, X. Jin, J. F. Holzman, F. Menard, K. Kim, *Conf. Proc. IEEE Eng. Med. Biol. Soc.* **2017**, 2017, 1599.
- [52] S. Das, F. Pati, Y. J. Choi, G. Rijal, J. H. Shim, S. W. Kim, A. R. Ray, D. W. Cho, S. Ghosh, *Acta Biomater.* **2015**, 11, 233.
- [53] Y. S. Zhang, A. Khademhosseini, *Science* **2017**, 356, eaaf3627.
- [54] W. J. Kim, H. S. Yun, G. H. Kim, *Sci. Rep.* **2017**, 7, 9.
- [55] A. J. Evinger, J. M. Jeyakumar, L. A. Hook, Y. Choo, B. R. Shephard, S. C. Presnell, *FASEB J.* **2013**, 27, 193.2.
- [56] L. D. Loozen, F. Wegman, F. Oener, W. J. Dhert, J. Alblas, *J. Mater. Chem. B* **2013**, 1, 6619.
- [57] M. Angelozzi, M. Miotto, L. Penolazzi, S. Mazzitelli, T. Keane, S. F. Badylak, R. Piva, C. Nastruzzi, *Mater. Sci. Eng., C* **2015**, 56, 141.
- [58] P. B. Malafaya, G. A. Silva, R. L. Reis, *Adv. Drug Delivery Rev.* **2007**, 59, 207.
- [59] C. McBeth, J. Lauer, M. Ottersbach, J. Campbell, A. Sharon, A. Sauer-Budge, *Biofabrication* **2016**.
- [60] C. G. Williams, A. N. Malik, T. K. Kim, P. N. Manson, J. H. Elisseeff, *Biomaterials* **2005**, 26, 1211.
- [61] A. D. Rouillard, C. M. Berglund, J. Y. Lee, W. J. Polacheck, Y. Tsui, L. J. Bonassar, B. J. Kirby, *Tissue Eng., Part C* **2011**, 17, 173.
- [62] N. E. Fedorovich, J. R. De Wijn, A. J. Verbout, J. Alblas, W. J. Dhert, *Tissue Eng., Part A* **2008**, 14, 127.
- [63] A. E. Jakus, A. L. Rutz, R. N. Shah, *Biomed. Mater.* **2016**, 11, 014102.
- [64] N. E. Fedorovich, W. Schuurman, H. M. Wijnberg, H. Prins, P. R. van Weeren, J. Malda, J. Alblas, W. J. A. Dhert, *Tissue Eng., Part C* **2012**, 18, 33.
- [65] H. Lee, S. Ahn, L. J. Bonassar, G. Kim, *Macromol. Rapid Commun.* **2013**, 34, 142.
- [66] N. E. Fedorovich, H. M. Wijnberg, W. J. A. Dhert, J. Alblas, *Tissue Eng., Part A* **2011**, 17, 2113.
- [67] T. T. Demirtas, G. Irmak, M. Gumusderelioglu, *Biofabrication* **2017**, 9, 035003.
- [68] G. Gao, T. Yonezawa, K. Hubbell, G. Dai, X. Cui, *Biotechnol. J.* **2015**, 10, 1568.
- [69] M. J. Sawkins, P. Mistry, B. N. Brown, K. M. Shakesheff, L. J. Bonassar, J. Yang, *Biofabrication* **2015**, 7, 035004.
- [70] M. A. Kuss, R. Harms, S. Wu, Y. Wang, J. B. Untrauer, M. A. Carlson, B. Duan, *RSC Adv.* **2017**, 7, 29312.
- [71] M. T. Poldervaart, B. Goversen, M. de Ruijter, A. Abbadessa, F. W. Melchels, F. C. Oner, W. J. A. Dhert, T. Vermonden, J. Alblas, *PLoS One* **2017**, 12, e0177628.
- [72] D. F. Duarte Campos, A. Blaeser, K. Buellesbach, K. S. Sen, W. Xun, W. Tillmann, H. Fischer, *Adv. Healthcare Mater.* **2016**, 5, 1336.
- [73] M. Du, B. Chen, Q. Meng, S. Liu, X. Zheng, C. Zhang, H. Wang, H. Li, N. Wang, J. Dai, *Biofabrication* **2015**, 7, 044104.
- [74] S. T. Bendtsen, S. P. Quinnell, M. Wei, J. *Biomed. Mater. Res., Part A* **2017**, 105, 1457.
- [75] X. Wang, E. Tolba, H. C. Schröder, M. Neufurth, Q. Feng, B. Diehl-Seifert, W. E. G. Müller, *PLoS One* **2014**, 9, e112497.

- [76] M. Neufurth, X. Wang, H. C. Schröder, Q. Feng, B. Diehl-Seifert, T. Ziebart, R. Steffen, S. Wang, W. E. G. Müller, *Biomaterials* **2014**, 35, 8810.
- [77] S. Wüst, M. E. Godla, R. Müller, S. Hofmann, *Acta Biomater.* **2014**, 10, 630.
- [78] K. C. Hung, C.-S. Tseng, L.-G. Dai, S.-h. Hsu, *Biomaterials* **2016**, 83, 156.
- [79] S. England, A. Rajaram, D. J. Schreyer, X. Chen, *Bioprinting* **2017**, 5, 1.
- [80] J. A. Burdick, C. Chung, X. Jia, M. A. Randolph, R. Langer, *Biomacromolecules* **2005**, 6, 386.
- [81] A. Skardal, J. Zhang, L. McCoard, S. Oottamasathien, G. D. Prestwich, *Adv. Mater.* **2010**, 22, 4736.
- [82] K. Yue, G. Trujillo-de Santiago, M. M. Alvarez, A. Tamayol, N. Annabi, A. Khademhosseini, *Biomaterials* **2015**, 73, 254.
- [83] B. J. Klotz, D. Gawlitta, A. J. Rosenberg, J. Malda, F. P. Melchels, *Trends Biotechnol.* **2016**, 34, 394.
- [84] M. P. Lutolf, J. L. Lauer-Fields, H. G. Schmoekel, A. T. Metters, F. E. Weber, G. B. Fields, J. A. Hubbell, *Proc. Natl. Acad. Sci. USA* **2003**, 100, 5413.
- [85] G. Gao, A. F. Schilling, K. Hubbell, T. Yonezawa, D. Truong, Y. Hong, G. Dai, X. Cui, *Biotechnol. Lett.* **2015**, 37, 2349.
- [86] J. H. Shim, J. Y. Kim, M. Park, J. Park, D. W. Cho, *Biofabrication* **2011**, 3, 034102.
- [87] M. Sadat-Shojai, M. Khorasani, A. Jamshidi, *Mater. Sci. Eng., C* **2015**, 49, 835.
- [88] J. Visser, F. P. W. Melchels, J. E. Jeon, E. M. van Bussel, L. S. Kimpton, H. M. Byrne, W. J. A. Dhert, P. D. Dalton, D. W. Huttmacher, J. Malda, *Nat. Commun.* **2015**, 6, 6933.
- [89] L. K. Narayanan, P. Huebner, M. B. Fisher, J. T. Spang, B. Starly, R. A. Shirwaiker, *ACS Biomater. Sci. Eng.* **2016**, 2, 1732.
- [90] R. Levato, J. Visser, J. A. Planell, E. Engel, J. Malda, M. A. Mateos-Timoneda, *Biofabrication* **2014**, 6, 035020.
- [91] F. Pati, T. Song, G. Rijal, J. Jang, S. W. Kim, D. Cho, *Biomaterials* **2015**, 37, 230.
- [92] J. Wang, M. Yang, Y. Zhu, L. Wang, A. P. Tomsia, C. Mao, *Adv. Mater.* **2014**, 26, 4961.
- [93] A. L. Boskey, *BoneKey Rep.* **2013**, 2, 447.
- [94] M. Yamada, M. Shiota, Y. Yamashita, S. Kasugai, *J. Biomed. Mater. Res., Part B* **2007**, 82B, 139.
- [95] M. Rismanchian, N. Khodaeian, L. Bahramian, M. Fathi, H. Sadeghi-Aliabadi, *Iran. J. Pharm. Res.* **2013**, 12, 437.
- [96] D. M. Smith, J. Cray James, J. L. E. Weiss, E. K. Dai Fei, S. Shakir, S. A. Rottgers, J. E. Losee, P. G. Campbell, G. M. Cooper, *Ann. Plast. Surg.* **2012**, 69, 485.
- [97] G. M. Cooper, E. D. Miller, G. E. DeCesare, A. Usas, E. L. Lensie, M. R. Bykowski, J. Huard, L. E. Weiss, J. E. Losee, P. G. Campbell, *Tissue Eng., Part A* **2010**, 16, 1749.
- [98] L. Nikkila, P. Viitanen, N. Ashammakhi, *J. Biomed. Mater. Res., Part B* **2009**, 89B, 518.
- [99] A. Do, A. Akkouch, B. Green, I. Ozbolat, A. Debabneh, S. Geary, A. Salem, *Ann. Biomed. Eng.* **2017**, 45, 297.
- [100] A. H. Zisch, M. P. Lutolf, J. A. Hubbell, *Cardiovasc. Pathol.* **2003**, 12, 295.
- [101] D. W. Thompson, J. T. Butterworth, *J. Colloid Interface Sci.* **1992**, 151, 236.
- [102] S. Bose, S. Tarafder, A. Bandyopadhyay, *Ann. Biomed. Eng.* **2017**, 45, 261.
- [103] S. H. Hwang, S. Y. Kim, S. H. Park, M. Y. Choi, H. W. Kang, Y. Seol, J. H. Park, D. Cho, O. K. Hong, J. G. Rha, S. W. Kim, *Otolaryngol. – Head Neck Surg.* **2012**, 147, 568.
- [104] A. Shafee, M. Kabiri, N. Ahmadbeigi, S. O. Yazdani, M. Mojtahed, S. Amanpour, M. Soleimani, *Stem Cells Dev.* **2011**, 20, 2077.
- [105] V. Sabapathy, S. Kumar, *J. Cell. Mol. Med.* **2016**, 20, 1571.
- [106] A. J. Engler, S. Sen, H. L. Sweeney, D. E. Discher, *Cell* **2006**, 126, 677.
- [107] E. D. F. Ker, A. S. Nain, L. E. Weiss, J. Wang, J. Suhan, C. H. Amon, P. G. Campbell, *Biomaterials* **2011**, 32, 8097.
- [108] J. Wang, L. Wang, X. Li, C. Mao, *Sci. Rep.* **2013**, 3, 1242.
- [109] C. L. Ross, M. Siriwardane, G. Almeida-Porada, C. D. Porada, P. Brink, G. J. Christ, B. S. Harrison, *Stem Cell Res.* **2015**, 15, 96.
- [110] L. Moroni, A. Nandakumar, F. B. de Groot, C. A. van Blitterswijk, P. Habibovic, *J. Tissue Eng. Regen. Med.* **2015**, 9, 745.
- [111] C. Ribeiro, V. Sencadas, D. M. Correia, S. Lanceros-Méndez, *Colloids Surf., B* **2015**, 136, 46.
- [112] A. Ito, K. Ino, M. Hayashida, T. Kobayashi, H. Matsunuma, H. Kagami, M. Ueda, H. Honda, *Tissue Eng.* **2005**, 11, 1553.
- [113] R. De Santis, U. D'Amora, T. Russo, A. Ronca, A. Gloria, L. Ambrosio, *J. Mater. Sci.: Mater. Med.* **2015**, 26, 1.
- [114] J. Su, Y. Zheng, H. Wu, *Lab Chip.* **2009**, 9, 996.
- [115] E. Tsuruga, H. Takita, H. Itoh, Y. Wakisaka, Y. Kuboki, *J. Biochem.* **1997**, 121, 317.
- [116] J. J. Klawitter, S. F. Hulbert, *J. Biomed. Mater. Res.* **1971**, 5, 161.
- [117] K. Whang, K. E. Healy, D. R. Elenz, E. K. Nam, D. C. Tsai, C. H. Thomas, G. W. Nuber, F. H. Glorieux, R. Travers, S. M. Sprague, *Tissue Eng.* **1999**, 5, 35.
- [118] I. Schwartz, B. P. Robinson, J. O. Hollinger, E. H. Szachowicz, J. Brekke, *Otolaryngol. – Head Neck Surg.* **1995**, 112, 707.
- [119] S. C. Skaalure, U. Akalp, F. J. Vernerey, S. J. Bryant, *Adv. Healthcare Mater.* **2016**, 5, 432.
- [120] M. S. Shoichet, R. H. Li, M. L. White, S. R. Winn, *Biotechnol. Bioeng.* **1996**, 50, 374.
- [121] R. Mishra, B. Basu, A. Kumar, *J. Mater. Sci.: Mater. Med.* **2009**, 20, 2493.
- [122] Z. Zhang, W. Chai, R. Xiong, L. Zhou, Y. Huang, *Biofabrication* **2017**, 9, 025038.
- [123] S. Bajada, I. Mazakova, J. B. Richardson, N. Ashammakhi, *J. Tissue Eng. Regen. Med.* **2008**, 2, 169.
- [124] R. Xue, J. Y. Li, Y. Yeh, L. Yang, S. Chien, *J. Orthop. Res.* **2013**, 31, 1360.
- [125] X. Hu, S. Park, E. S. Gil, X. Xia, A. S. Weiss, D. L. Kaplan, *Biomaterials* **2011**, 32, 8979.
- [126] N. E. Fedorovich, M. H. Oudshoorn, D. van Geemen, W. E. Hennink, J. Alblas, W. J. A. Dhert, *Biomaterials* **2009**, 30, 344.
- [127] N. Ashammakhi, S. Ahadian, I. Pountos, S. Hu, N. Tellisi, S. Ostrovidov, M. Dokmeci, A. Khademhosseini, *Biomed. Microdev.* **2018**.
- [128] R. K. Jain, P. Au, J. Tam, D. G. Duda, D. Fukumura, *Nat. Biotechnol.* **2005**, 23, 821.
- [129] A. S. Goldstein, T. M. Juarez, C. D. Helmke, M. C. Gustin, A. G. Mikos, *Biomaterials* **2001**, 22, 1279.
- [130] H. Bae, A. S. Puranik, R. Gauvin, F. Edalat, B. Carrillo-Conde, N. A. Peppas, A. Khademhosseini, *Sci. Transl. Med.* **2012**, 4, 160ps23.
- [131] Y. Chen, R. Lin, H. Qi, Y. Yang, H. Bae, J. M. Melero-Martin, A. Khademhosseini, *Adv. Funct. Mater.* **2012**, 22, 2027.
- [132] C. Correia, W. L. Grayson, M. Park, D. Hutton, B. Zhou, X. E. Guo, L. Niklason, R. A. Sousa, R. L. Reis, G. Vunjak-Novakovic, *PLoS One* **2011**, 6, e28352.
- [133] S. Stegen, N. van Gastel, G. Carmeliet, *Bone* **2015**, 70, 19.
- [134] J. Baldwin, M. Antille, U. Bonda, E. M. De-Juan-Pardo, K. Khosrotehrani, S. Ivanovski, E. B. Petcu, D. W. Huttmacher, *Vasc. Cell* **2014**, 6, 13.
- [135] M. I. Santos, R. E. Unger, R. A. Sousa, R. L. Reis, C. J. Kirkpatrick, *Biomaterials* **2009**, 30, 4407.
- [136] F. Kawecki, W. P. Clafshenkel, F. A. Auger, J. Bourget, J. Fradette, R. Devillard, *Biofabrication* **2018**, 10, 035006.
- [137] J.-M. Bourget, O. Kérouédan, M. Medina, M. Rémy, N. B. Thébaud, R. Bareille, O. Chassande, J. Amédée, S. Catros, R. Devillard, *Biomed. Res. Int.* **2016**, 2016, 3569843.
- [138] D. B. Kolesky, R. L. Truby, A. S. Gladman, T. A. Busbee, K. A. Homan, J. A. Lewis, *Adv. Mater.* **2014**, 26, 3124.

- [139] N. E. Fedorovich, R. T. Haverslag, W. J. A. Dhert, J. Alblas, *Tissue Eng., Part A* **2010**, 16, 2355.
- [140] M. Kazemzadeh-Narbat, J. Rouwkema, N. Annabi, H. Cheng, M. Ghaderi, B. H. Cha, M. Aparnathi, A. Khalilpour, B. Byambaa, E. Jabbari, A. Tamayol, A. Khademhosseini, *Adv. Healthcare Mater.* **2017**, 6, 1601122.
- [141] J. Ma van den Beucken, J. J. P. Jeroen, F. Yang, S. K. Both, F. Cui, J. Pan, J. A. Jansen, *Tissue Eng., Part C* **2011**, 17, 349.
- [142] M. J. Barron, J. Goldman, C. Tsai, S. W. Donahue, *Int. J. Biomater.* **2012**, 2012, 1.
- [143] N. V. Rodionova, V. S. Oganov, *Adv. Space Res.* **2003**, 32, 1477.
- [144] W. Lattanzi, N. Alves, P. Morouco, *Front. Bioeng. Biotechnol.* **2017**, 5.
- [145] A. Atala, F. K. Kasper, A. G. Mikos, *Sci. Transl. Med.* **2012**, 4, 160rv12.
- [146] F. Obregon, C. Vaquette, S. Ivanovski, D. W. Huttmacher, L. E. Bertassoni, *J. Dent. Res.* **2015**, 94, 1435.
- [147] D. Mohammadi, *Lancet* **2017**, 390, 1823.
- [148] D. Confalonieri, A. Schwab, H. Walles, F. Ehlicke, *Tissue Eng., Part B Rev.* **2017**.
- [149] K. B. Hellman, *Topics in Tissue Engineering*, Vol. 4 (Eds: N. Ashammakhi, R. Reis, F. Chiellini), Oulu University, Oulu, Finland **2008**.
- [150] A. E. Jakus, A. L. Rutz, S. W. Jordan, A. Kannan, S. M. Mitchell, C. Yun, K. D. Koube, S. C. Yoo, H. E. Whiteley, C. Richter, R. D. Galiano, W. K. Hsu, S. R. Stock, E. L. Hsu, R. N. Shah, *Sci. Transl. Med.* **2016**, 8, 358ra127.
- [151] M. Orciani, M. Fini, R. Di Primio, M. Mattioli-Belmonte, *Front. Bioeng. Biotechnol.* **2017**, 5, 17.
- [152] S. J. Hollister, C. L. Flanagan, D. A. Zopf, R. J. Morrison, H. Nasser, J. J. Patel, E. Ebrahmzadeh, S. N. Sangiorgio, M. B. Wheeler, G. E. Green, *Ann. Biomed. Eng.* **2015**, 43, 774.
- [153] N. Ashammakhi, S. Ahadian, M. A. Darabi, M. El Tahchi, J. Lee, K. Suthiwanich, A. Sheikhi, M. R. Dokmeci, R. Oklu, A. Khademhosseini, *Adv. Mater.* **2018**.
- [154] D. Raviv, W. Zhao, C. McKnelly, A. Papadopoulou, A. Kadambi, B. Shi, S. Hirsch, D. Dikovsky, M. Zyracki, C. Olguin, R. Raskar, S. Tibbitts, *Sci. Rep.* **2015**, 4, 7422.
- [155] N. Ashammakhi, S. Ahadian, F. Zengjie, K. Suthiwanich, F. Lorestani, G. Orive, S. Ostrovidov, A. Khademhosseini, *Biotechnol. J.* **2018**.
- [156] S. Tibbitts, *Architect. Des.* **2014**, 84, 116.
- [157] A. S. Gladman, E. A. Matsumoto, R. G. Nuzzo, L. Mahadevan, J. Lewis, *Nat. Mater.* **2016**, 15, 413.
- [158] Q. Ge, A. H. Sakhaei, H. Lee, C. K. Dunn, N. X. Fang, M. L. Dunn, *Sci. Rep.* **2016**, 6, 31110.
- [159] Y.-C. Li, Y. S. Zhang, A. Akpek, S. R. Shin, A. Khademhosseini, *Biofabrication* **2016**, 9, 012001.
- [160] S. Wang, J. M. Lee, W. Y. Yeong, *Int. J. Bioprint.* **2015**.
- [161] N. Ashammakhi, O. Kaarela, *J. Craniofac. Surgery* **2017**, 28, 1647.
- [162] R. Censi, W. Schuurman, J. Malda, G. di Dato, P. E. Burgisser, W. J. A. Dhert, C. F. van Nostrum, P. di Martino, T. Vermonden, W. E. Hennink, *Adv. Funct. Mater.* **2011**, 21, 1833.
- [163] N. Jackson, F. Stam, *J. Appl. Polym. Sci.* **2015**, 132, n/a.
- [164] G. Giani, S. Fedi, R. Barbucci, *Polymers* **2012**, 4, 1157.
- [165] M. Sabzi, M. Babaahmadi, M. Rahnama, *ACS Appl. Mater. Interface.* **2017**.
- [166] G. Mattei, C. Ferretti, A. Tirella, A. Ahluwalia, M. Mattioli-Belmonte, *Sci. Rep.* **2015**, 5, 10778.
- [167] M. Mattioli-Belmonte, G. Vozzi, Y. Whulanza, M. Seggiani, V. Fantauzzi, G. Orsini, A. Ahluwalia, *Mater. Sci. Eng., C* **2012**, 32, 152.
- [168] S. K. Khorshidi, *J. Biomed. Mater. Res. A* **2017**.
- [169] K. Takahashi, S. Yamanaka, *Cell* **2006**, 126, 663.
- [170] E. S. Bishop, S. Mostafa, M. Pakvasa, H. H. Luu, M. J. Lee, J. M. Wolf, G. A. Ameer, T. He, R. R. Reid, *Genes Dis.* **2017**, 4, 185.
- [171] J. Malda, J. Visser, F. P. Melchels, T. Jüngst, W. E. Hennink, W. J. A. Dhert, J. Groll, D. W. Huttmacher, *Adv. Mater.* **2013**, 25, 5011.